Master Thesis
TVVR 21/5017

Wave Damping by Vegetation at Bunkeflo Salt Meadows

Applying an empirical model based on plant biomass

Charlie van Houwelingen

Timothy Ley

Division of Water Resources Engineering
Department of Building and Environmental Technology
Lund University

Wave Damping by Vegetation at Bunkeflo Salt Meadows

Applying an empirical model based on plant biomass

By:
Charlie van Houwelingen
Timothy Ley

Master Thesis

Division of Water Resources Engineering
Department of Building & Environmental Technology
Lund University
Box 118
221 00 Lund, Sweden

Title page image: *Bunkeflo salt meadows - April 2, 2021. Creator Timothy Ley.*

Water Resources Engineering
TVVR- 21/5017
ISSN 1101-9824

Lund 2021
www.tvrl.lth.s

Master Thesis

Division of Water Resources Engineering
Department of Building & Environmental Technology
Lund University

Swedish title:	Vågdämpning från Vegetation vid Bunkeflo Strandängar – Tillämpning av en empirisk model baserad på biomassa
English title:	Wave Damping by Vegetation at Bunkeflo Salt Meadows – Applying an empirical model based on plant biomass
Author(s):	Charlie van Houwelingen Timothy Ley
Supervisor(s):	Björn Almström, Caroline Hallin and Emanuel Schmidt
Examiner:	Magnus Larson
Language	English
Year:	2021
Keywords:	Coastal protection; nature-based solutions; salt marshes; salt meadows; sea level rise; wave damping

Acknowledgements

We wish to express our deepest gratitude to our supervisors Caroline Hallin, Björn Almström and Emanuel Schmidt for their dedication and invaluable support. The topic of the thesis required a great deal of innovative ideas and solutions along the way, many of which we would never have thought of on our own. Through all of our discussions, our supervisors shared knowledge, experience and understanding which we will always be thankful for and bring with us into the future. Caroline and Björn kept sparking our interest with ideas throughout the process and were always available. Emanuel gave us valuable insights into the real world of the coastal engineering and helped us identify the most valuable aspects of our work. We would also like to thank Pål Axel Olsson for his help in designing our field study.

This master thesis has been a collaboration between Lund Technical University (LTH) and the consultancy company Sweco. We appreciate and want to thank them for helping us during the field survey by giving us access to their geo-laboratory.

Finally, we wish to thank our family, friends and loved ones. This term has been exceptional in many ways and working through the pandemic has been challenging at times. Your love and understanding has been more important than you will ever know. Thank you.

Abstract

Future sea level rise due to climate change increases the risk of coastal flooding and thus necessitates the building of dikes and other protective structures. Coastal vegetation can reduce the impact of waves on such structures by dissipating wave energy and hence reduce incoming wave heights. This thesis attempts to quantify the wave damping by vegetation at Bunkeflostrand (southern Sweden), by using an empirical method based on plant biomass. An analysis is made of how the damping is influenced by the type of vegetation and by the hydrodynamic conditions.

Through field surveys in combination with geographical information system (GIS) software, the area was classified into several vegetation types whose biomass and vegetation height were measured and used as an input to the model. The influence of vegetation characteristics and hydrodynamic conditions were studied in hypothetical cases using MATLAB. As a case study, wave damping over four transects at Bunkeflostrand was estimated by applying the biomass method to the classified maps using a script in Python.

The results showed that reed reduced wave heights the most when the water depth exceeded 0.5 m. In shallower water, high grass dampened the most. The relationship between water depth and vegetation height was especially important, where emergent vegetation dampened waves better. Over the salt meadows, the calculations showed wave height reductions between 65.6 % and 94.6 %, depending on transect and scenario. Compared to other studies, the biomass method tends to overestimate wave damping. For this reason, it is not recommended for use in design calculations. However, it is recommended to maintain a buffer zone of vegetation in front of dikes, both for the wave damping effect and for other ecosystem services that such zones provide.

Sammanfattning

Havsnivåhöjning till följd av klimatförändringar ökar risken för översvämningar vid kusten och nödvändiggör konstruktionen av skyddsvallar och andra kustskyddsåtgärder. Vegetation vid kusten kan vara en del i dessa skyddsåtgärder genom att reducera våghöjden på de inkommande vågorna. Detta examensarbete kvantifierar vågdämpningen från vegetation vid Bunkeflo strandängar (Malmö) med hjälp av en empirisk metod baserat på växters biomassa och höjd. En analys görs av hur dämpningen påverkas av typen av vegetation och de hydrodynamiska förhållandena på platsen.

Fältstudier i kombination med ett geografiskt informationssystem (GIS) användes för att klassificera vegetationen vars massa och höjd mättes och användes som in-data i modellen. Påverkan av vegetationskaraktäristika och hydrodynamiska förhållanden studerades i hypotetiska fall med hjälp av MATLAB. I en fallstudie av Bunkeflo strandängar gjordes beräkningar med biomassa-metoden längs fyra transekter vid Bunkeflostrand genom ett script i Python baserat på data från de klassificerade kartorna.

Resultaten visade att vass är den vegetationstyp som dämpar vågor mest när vattendjupet överstiger 0.5 m. I grundare vatten dämpade högt gräs mer. Relationen mellan vattendjup och vegetationshöjd identifierades som särskilt viktig, där vegetation som är ovan vattenytan dämpade vågor mer. Beräkningarna i fallstudien visade att strandängarna dämpar vågor med 65,6 % and 94,6 %, beroende på transekt och scenario. Jämfört med andra studier verkar biomassa metoden överskatta vågdämpning. Därav rekommenderas det inte att använda denna metod för att designa skyddsvallar. Emellertid rekommenderas det att bevara eller etablera vegetation framför vallar, både för dess vågdämpningsfunktion och för värdet av andra ekosystemtjänster från dessa zoner.

Notations

Table 1. List of symbols used in this thesis.

Symbol	Parameter	Unit
β	Damping coefficient	-
C_d	Bulk drag coefficient	-
W_{dry}	Dry weight	g/m^2
h	Water depth	m
h_{veg}	Vegetation height	m
H	Wave height	m
H_0	Wave height at shoreline	m
H_i	Incident wave height	m
HB	Hydraulic biomass	g/m^3
L	Wavelength	m
LR	Length relation	-
L_{veg}	Transect length	m
n	Segment number	-
SB	Standing biomass	g/m^2
SR	Submerged ratio	-
x	Cross shore distance	m

Table 2. List of abbreviations used in this thesis.

Abbreviation	Meaning
GH	High grass
MH	High meadow
RH	High reed
RL	Low reed

Contents

1 Introduction

Across the globe, coastal protection will become increasingly important as a consequence of climate change. About 10 % of the global population live in low-lying coastal areas, and 15 of the 23 mega cities in the world are coastal (Blackburn et al., 2019). As climate change progresses, causing further sea level rise, human settlements thus become increasingly vulnerable both to a gradually increasing water level as well as to natural disasters such as coastal flooding during storms, which are exacerbated due to a higher water level.

Traditionally, the response to such risks has been to construct dikes, sea walls, or moveable barriers such as the Thames Barrier in London. While such so-called "grey" structures may be effective, they can be costly to build and risk causing or exacerbating erosion problems elsewhere (Spalding et al., 2014). In recent decades, nature-based solutions, which use and manage natural systems to solve societal problems (Cohen-Shacham et al., 2016), have been gaining attention. Such "green" structures can be used in combination with grey structures in hybrid systems in order to gain the benefits provided by both (Sutton-Grier et al., 2015).

Compared to traditional engineering solutions, nature-based solutions have the advantage that they may adapt to environmental changes since they consist at least partly of living elements, and that they may yield synergistic benefits such as increased biodiversity and providing ecosystem services (Cohen-Shacham et al., 2016).

An example is wave damping by coastal vegetation. Coastal marshes are some of the most productive ecosystems in the world, providing habitat to a wide range of plants, birds, mammals, amphibians, and fishes (Millennium Ecosystem Assessment, 2005). They provide ecosystem services such as water treatment of runoff from land, prevention of coastal erosion by stabilizing sediments and, crucially, by reducing wave heights (Gedan et al., 2011; Millennium Ecosystem Assessment, 2005; Shepard et al., 2011). They thus provide a buffer zone that reduces the wave energy that engineered structures are subjected to. Hence, construction and maintenance costs may be reduced while simultaneously providing the other ecosystem services outlined above. Additionally, salt marshes may be able to adapt to sea level rise by trapping sediments and thus growing vertically, highlighting their potential as climate change adaptation measures (Kirwan et al., 2016).

If the design of a dike is going to take wave damping from vegetation into account, it is necessary to quantify the wave damping that can be expected. This is

complicated since the processes involved are not fully understood and can often depend on the specific plant species (Möller, 2006). Recently, a method has been developed that estimates the wave damping based on vegetation biomass (Maza, 2020). This report will use this method to estimate wave damping from vegetation at the study site of Bunkeflo salt meadows in southern Sweden.

1.1 Aim and Research Questions

The aim of this thesis is to investigate and quantify the wave damping of the salt meadows at Bunkeflostrand and to put this function into a wider context of coastal protection. It will look at short hypothetical vegetation field segments to elucidate the influence of specific parameters. As a case study, it will also investigate damping along transects at Bunkeflostrand for different scenarios of extreme water levels combined with high waves.

The main objective is to develop a wave damping computation framework based on the biomass method by Maza et al. (2020) that can be applied to field conditions for different types of vegetation. This thesis will thereby attempt to answer the following questions:

- How much wave damping can be expected from the salt meadows at Bunkeflostrand?
- What are the most important parameters influencing wave damping, related to hydrodynamic conditions and vegetation characteristics at Bunkeflo salt meadows?

Based on these findings, recommendations will be given as to how the salt meadows can be managed to increase their wave damping functionality.

1.2 Method Summary

The first step of the data collection process was to conduct field studies to acquire input parameters related to vegetation characteristics and spatial distribution of vegetation types at Bunkeflo salt meadows. In combination with hydrodynamic and geographical data, a spatial analysis was performed in GIS-software to define data points along transects at the site. Scripts in Python and MATLAB were then written and used to perform the wave damping calculations. These calculations were also made for hypothetical cases to analyse the influence of different model parameters. An analysis of the results in relation to previous studies was made to determine the reliability of the results.

1.3 Structure

In section 2 (*Study Site*) a general background to the study site Bunkeflostrand is given. Section 3 (*Theory*) introduces the basic theory behind wave damping by vegetation, explains common analytical models of wave damping and introduces the model that will be used in this report. An overview of recent studies on wave damping by vegetation is also provided. Section 4 (*Methods)* details the methods of this thesis used to achieve the objectives, followed by the results in section 5 (*Results*). These sections (4 and 5) will look at both hypothetical cases of idealized vegetation types found at Bunkeflostrand as well as the case study of the salt meadows along transects. In section 6 (*Discussion*) the results are evaluated, discussed, and put into a larger context of coastal protection in the face of climate change. Section 7 (*Conclusions*) summarizes the report and gives recommendations based on the findings.

2 Site Description

Bunkeflostrand is a small residential area located in the southwestern corner of the municipality of Malmö, just south of the Öresund bridge (Figure 1). The salt meadows to the west of Bunkeflostrand have been used for grazing since the Bronze age (Länsstyrelsen Skåne, n.d.). Periodical inundations of seawater together with the long history of grazing has created an area of high biodiversity, with around 300 plant species and 450 species of birds, frogs, and insects (Ibid.). The area is an important resting place for migrating birds and has been a nature reserve since 2007 (Ibid.). As a consequence of the industrialization of agriculture, grazing declined in the 20th century, causing parts of the salt meadows to become overgrown with reeds and tall grasses. This is a common problem for many similar habitats (Länsstyrelsen Västra Götaland, 2020). For this reason, part of the management strategy of Bunkeflo salt meadows is to ensure that large parts of the area remain open through grazing (Malmö stad, n.d.).

Technically, the habitat is classified as an Atlantic salt meadow (*Glauco-Puccinellietalia maritimae*) (Naturvårdsverket, 2011). However, since the tidal impact and salinity levels are relatively low, the habitat shares characteristics with the neighboring Boreal Baltic coastal meadows found on the east coast of Sweden (Doody et al., 2008).

Although human settlement in the area is probably at least as old as grazing by livestock, the first residential areas were built in the 1920's. The population was around 400 in the 1930's (Emanuelson & Holmquist, 2019). In recent decades, the population has grown dramatically, with 5000 inhabitants in 2000, increasing to 13000 in 2015 (SCB, 2021). At the same time, Bunkeflostrand is a topographically low-lying coastal area, exposed to the Öresund strait in the west and hence vulnerable to rising sea levels. This is especially true for the area called Strandhem, located between 50 and 100 m from the shoreline (Figure 1). After a storm in January 2017, a water level of 145 cm above mean sea level was recorded at Klagshamn, leading to flooding in Bunkeflostrand (Simonsson & Liljedahl, 2017). Although the damages were minor, projected sea level rise in the 21st century means future storm surges could cause substantial damage (Malmö Stadsbyggnadskontor, 2008).

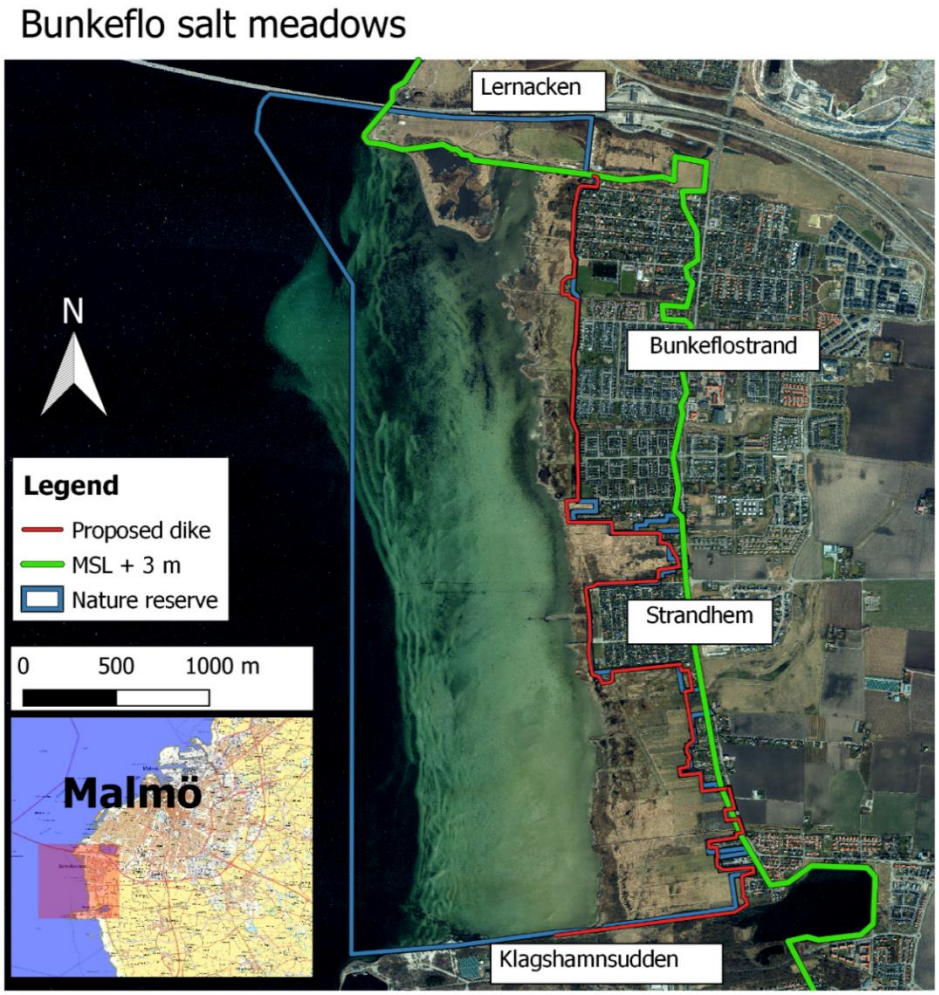

Figure 1. Overview of Bunkeflostrand and its salt meadows. Includes proposed location of a future dike as well as a line demarcating 3 m above mean sea level. The nature reserve is the area enclosed by the blue line. Dike location from: Strategi mot extrema högvatten i Malmö (Sweco, 2017). Map data from: Ortofoto RGB 0.25 m latest, © Lantmäteriet. Nature reserve boundaries from: Naturreservat © Naturvårdsverket.

As part of its climate adaptation strategy, the city of Malmö recommends that all new buildings in the municipality have their lowest level at 3 m above mean sea level (Malmö stad, 2020). A substantial part of Bunkeflostrand lies below this level, as is shown by the green line in Figure 1. Therefore, it has been proposed that a dike be constructed to protect Bunkeflostrand from future coastal flooding (Almström et al., 2017; Malmö Stadsbyggnadskontor, 2008). The proposed location of the dike is shown by the red line in Figure 1. At Strandhem, a sea dike was built in 1988 to protect against coastal flooding (Jönsson & Jönsson, 2015). The dike is

roughly 2.4 m above mean sea level. In order to withstand future sea level rise, it may need to be elevated.

The design of a sea dike depends on the hydrodynamic forces it is meant to withstand, where the main factors to consider are water levels and wave heights (EurOtop, 2018). Waves can cause overtopping and structural damage to a dike, which makes it important to know what wave heights the dike will be subjected to. As mentioned in section 1, a vegetated foreshore can reduce wave heights. The salt meadows at Bunkeflostrand thus provide a valuable buffer against wave action, but to include their effect when designing a dike requires quantifying the wave damping.

3 Theory

This section will provide a general background on the study of wave damping by vegetation, as well as the most common parameters studied. An overview of methods used to model wave damping is then presented, followed by an explanation of the method used to calculate the wave damping in this report.

3.1 Theoretical Background

Waves propagating through vegetation fields lose energy by performing work on the plant stems (Dalrymple et al., 1984). The resistance of the plants to the water flow causes drag, which is the fundamental reason vegetation dampens waves. As wave energy dissipates, the wave height is reduced, which is depicted in Figure 2 below.

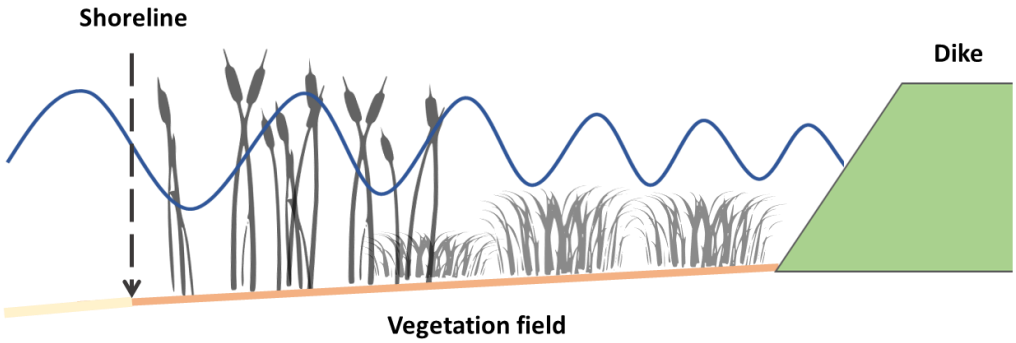

Figure 2. Wave damping by vegetation seaward of a dike. The water level is above the mean sea level to illustrate how vegetation can reduce wave hights in extreme water level scenarios. The dashed arrow indicates the position of the shoreline at mean sea level.

Wave damping by vegetation is a complex process governed by hydrodynamic conditions, such as wave height, wave period and water depth, and plant characteristics, such as vegetation height, stem stiffness and density (Anderson et al., 2011; Shepard et al., 2011). At present, there is no existing modelling framework to calculate wave damping from vegetation that is generally applicable to a broad variety of plant species and diverse hydrodynamic conditions. Furthermore, models often require calibration (van Veelen, 2020), which in many cases may not be possible due to infrequency of extreme events and/or limited resources to conduct laboratory studies. However, in recent years several different calculation methods

have been proposed and developed that may achieve satisfactory results depending on the required scale and resolution of the hydrodynamics.

A seemingly simple way to account for damping from vegetation is by introducing an increased bottom friction factor (e.g. Augustin et al., 2009; Möller et al., 1999; Wamsley et al., 2009). Whilst this method may be promising and satisfactory for predicting large-scale wave and storm surge conditions, small-scale hydrodynamic effects lack in accuracy and detail (Yang & Irish, 2018).

As an alternative, a majority of studies have opted to express the wave damping inflicted by plants as a drag force determined by an empirical bulk drag coefficient (C_d) (Anderson et al., 2011). This approach better describes the physical processes within the vegetation by considering plant specific characteristics such as stem diameter, density and flexibility (Suzuki et al., 2012). Furthermore, by calibration of the bulk drag coefficient, additional processes not yet fully understood can be accounted for (Suzuki et al., 2012). Among the first analytical wave height attenuation equations developed from these physical principles were derived by Dalrymple et al. (1984) and Kobayashi et al. (1993). These two studies have laid an important theoretical foundation for many studies to follow. Based on linear wave theory and the laws of energy conservation, Dalrymple et al. (1984) derived the following damping equation:

$$\frac{H(x)}{H_0} = \frac{1}{1 + \beta x} \tag{1}$$

where $H(x)$ is the wave height at a distance x into the vegetation field, H_0 is the wave height at the seaward limit of the vegetation field ($H(x = 0)$) and β is the damping coefficient which is a function of the bulk drag coefficient (C_d).

Kobayashi et al. (1993) derived an alternative exponential damping equation based on the conservation of momentum instead:

$$\frac{H(x)}{H_0} = e^{-\beta x} \tag{2}$$

These equations were originally developed and validated by laboratory experiments of monochromatic waves passing through rigid homogeneous cylinders. Consequently, the equations are based on the premisses that the bottom is horizontal and that the waves are non-breaking and regular. Since then, attention has been focused to develop more realistic and complete methods to calculate the damping coefficient. Additional hydrodynamic parameters have been added and detailed plant characteristics have been quantified further. In addition to these advancements, Mendez & Losada (2004) further developed Eq. (1) by Dalrymple et

al. (1984) to take into account shoaling and breaking for sloping foreshores. In summary, many steps have been taken in recent years to improve the accuracy of these analytical equations.

3.2 Key Parameters

Several studies point to the relative height of the vegetation compared to the water depth as being an important factor, especially when the vegetation is submerged (e.g. Augustin et al., 2009; Möller et al., 1999; Maza et al., 2015; Rupprecht et al., 2017). The explaining mechanism has been suggested to be that wave orbital velocities are higher closer to the water surface, and when the vegetation covers the entire water column it effectively interacts with the entire velocity profile, including the highest velocities (Augustin et al., 2009). Other parameters influencing wave damping are the ratios between incident wave height and water depth (Garzon et al., 2019; Möller et al., 1999; Wu & Cox, 2015), the type of vegetation and its density (Bouma et al., 2010; Möller, 2006) and the wave period (Garzon et al., 2019). However, when it comes to incident wave height, some studies report that higher incident waves cause greater damping (Möller et al., 2011) while others report a decreasing damping effect when incident waves are higher (Maza et al., 2015).

Another plant characteristic of interest, besides vegetation height, is flexibility. Several laboratory studies have investigated species of different stem flexibility and found that for low water levels and wave heights stiff vegetation damps better than flexible vegetation (e.g. Maza et al., 2015; Rupprecht et al., 2017; van Veelen et al., 2020), which may be caused by the greater drag force generated by stiff vegetation (Bouma et al., 2010). However, when water levels and waves are high, both stiff and flexible vegetation may simply bend over, and stiff vegetation has also been observed to experience stem breakage under storm surge conditions (Rupprecht et al., 2017). This highlights the importance of understanding how hydrodynamic conditions may affect vegetation characteristics.

Despite differences in wave damping capacity between flexible and non-flexible species, Bouma et al. (2010) noticed a similar wave damping capacity when expressed per unit biomass. This indicates that biomass can be used as a proxy for wave damping even for species with different biomechanical properties. A relation between wave damping and biomass has also been observed in other studies (e.g. Maza et al., 2015; Maza et al., 2020). Maza et al (2020) were able to demonstrate that biomass could be linearly related to wave damping when including other hydrodynamic conditions such as wave height and water depth. This approach

would enable the calculation of wave damping from habitats with many different species, where drag forces and vegetation characteristics vary greatly.

3.3 Field and Laboratory Studies

The study of wave damping can be broadly divided into two types, namely field studies and laboratory flume studies.

Field studies are conducted by placing wave gauges along one or more transects in the field and measuring the wave height as waves travel landwards. This provides data from real wave conditions acting on in situ vegetation, interacting with factors such as bathymetric features and currents. However, while being more realistic than laboratory studies, it may also be harder to disentangle the different effects that may affect wave propagation. For instance, wave damping can be influenced by coastline morphology (Möller et al., 2011), tidal currents (Garzon et al., 2019; Paquier et al., 2017; Paul et al., 2012), and seasonal variations in vegetation cover (Möller & Spencer, 2002; Paul & Amos, 2011). However, it is well established that the presence of vegetation significantly reduces wave heights (Anderson et al., 2011; Gedan et al., 2011; Shepard et al., 2011).

Laboratory studies are conducted by placing either real vegetation or artificial mimics in a flume and then generating waves and analyzing the results. This allows researchers to study how each parameter influences the damping by studying their effect in isolation (Anderson et al., 2011). Compared to living vegetation, the main advantages of using mimics is that they are relatively cheap to obtain, are scalable and don't require maintenance (Maza et al., 2020). While useful for studying factors such as the effects of flexibility, they may represent real vegetation poorly, which is the main advantage of using real vegetation.

3.4 Wave Damping Models

Building on analytical equations presented in section 3.1, extensions to numerical hydrodynamic process models have been developed, such as SWAN-VEG (Suzuki et al., 2012) and XBeach-VEG (Rooijen et al., 2015). However, these models still rely on calibration of the bulk drag coefficient for each vegetation type depending on the hydrodynamic condition (Suzuki et al., 2012).

Due to the complex nature of calculating the bulk drag coefficient, a number of alternative methods to model wave damping have been presented in recent years. Maza et al. (2015) developed a 3D-model of mangroves and concluded that simulating the actual geometry of plants was superior in predicting wave forces,

compared to a drag force approximation. This method is useful when studying detailed local effects, but the computational costs are high (Maza et al., 2015). In response to the complexity of currently available wave damping models, Foster-Martinez et al. (2020) developed a GIS-toolbox enabling classification of vegetation wave damping zones depending on inundation level and vegetation biomass. In order to avoid calibration of the drag coefficient, Foster-Martinez et al. (2020) has provided a damping coefficient selection chart based on results from previous field studies. This makes the model easy to use and efficient to apply to large-scale study areas. However, depending on how well the damping coefficients found in field studies match the real site conditions, the uncertainty of the results may be high.

Ultimately, it would be desirable to develop a method that is of sufficient hydrodynamic resolution and requires less calibration by extensive field and laboratory studies. This objective was sought after in a study by Maza et al. (2020) mentioned in section 3.2. By identifying biomass as a key parameter in determining the wave damping for different plant species and wave conditions, Maza (2020) concluded that the method (hereafter referred to as the "biomass method") may represent a major advancement in modelling wave damping by vegetation.

3.5 Biomass Method

Based on the wave decay equation by Dalrymple et al. (1984) (Eq (1)), Maza et al. (2020) used standing biomass as a proxy for the actual drag force. Consequently, the bulk drag coefficient is not used and therefore does not require calibration. This is a major benefit since the drag coefficient is often unknown, especially for complex real-world applications (Maza, 2020). Furthermore, other parameters related to geometrical and biomechanical properties of the plant are not required, with the exception of vegetation height.

The method was developed and validated by conducting flume experiments for real vegetation collected from estuaries in Cantabria (Spain). Four common saltmarsh species (*Spartina maritima, Salicornia sp., Halimione sp.* and *Juncus sp.*) were placed in the flume, creating a 9 m long vegetation field. Each plant species was tested for three meadow densities (100%, 50% and 0%) by cutting the vegetation between test-runs. 12 wave conditions were run for: depth = 0.20, 0.30 and 0.40 m; wave height = 0.08 - 0.18 m and wave period 1.5 - 4 s. Both random and regular wave conditions were tested, but so far only regular wave conditions have been presented by Maza (2020).

Based on the results from their flume experiments with varying wave conditions, Maza et al. (2020) created a common relationship for all wave conditions by

introducing the so-called hydraulic biomass (HB). The relation between the damping coefficient and the hydraulic biomass was found to be:

$$\beta = 9.2 * 10^{-4} * HB + 0.10 \quad (3)$$

The hydraulic biomass is the actual volume of the biomass interacting with the flow (i.e. the submerged parts of the plant), that is in turn determined by the water depth (h), the incident wave height (H_i), the wavelength (L) and the unit length of the vegetation field (L_{veg}).

$$HB = \frac{SB}{h} * \frac{L_{veg}}{L} * \frac{H_i}{h} \quad (4)$$

The hydraulic biomass is related to the standing biomass (SB), which is defined by Maza et al. (2020) as:

$$SB = \frac{W_{dry}}{h_{veg}} * \min\{h_{veg}, h\} * SR \quad (5)$$

Where W_{dry} is the dry biomass in g/m^2, and the submergence ratio (SR) is defined as:

$$SR = \frac{h_{veg}}{h}, \quad SR = 1 \; if \; h_{veg} > h \quad (6)$$

Figure 3 bellow illustrates how water depth and vegetation height effect the submergence ratio.

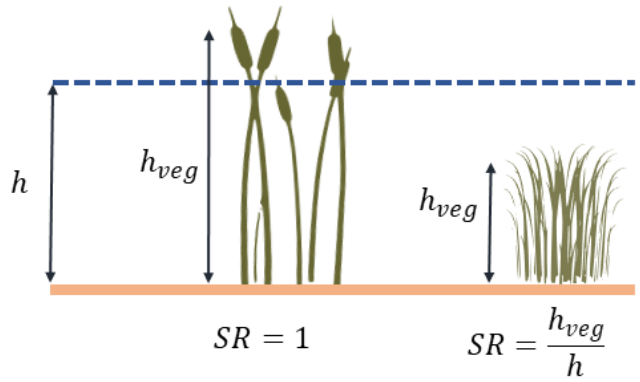

Figure 3. The illustration shows how the submergence ratio can vary between species depending on the water depth.

It is important to highlight that the study by Maza et al. (2020) is in the process of being published. Therefore, the description of the method in this report may be incomplete and subject to change once the final article is published.

4 Methods

Wave damping by vegetation was calculated based on the empirical equations derived by Maza et al. (2020), with some required modifications for applicability to field conditions (see section 4.4.3 and Appendix A1). Vegetation classes were created based on the different plant communities present at Bunkeflo salt meadows and the height and biomass were measured for four of the vegetation classes. Three hydrodynamic scenarios were defined with a water level corresponding to the 100-year flood level for the years 2021, 2050 and 2100. The water levels were combined with the highest possible wave heights in the area, which were calculated from a wave height time series. Thereafter, data from the field study was processed with GIS-software. Transects were created in the software and vegetation- and topographical data was extracted along these lines. The calculations were performed by running a script created in Python (Appendix A5.1). Finally, the results are presented both for the hypothetical cases (section 5.3) and for the case study (section 5.4). The purpose of the hypothetical cases is to make the results easier to compare with other studies and to simplify parameter analysis. Figure 4 below is a brief overview of the work process. Detailed descriptions of each step are given in the sections below.

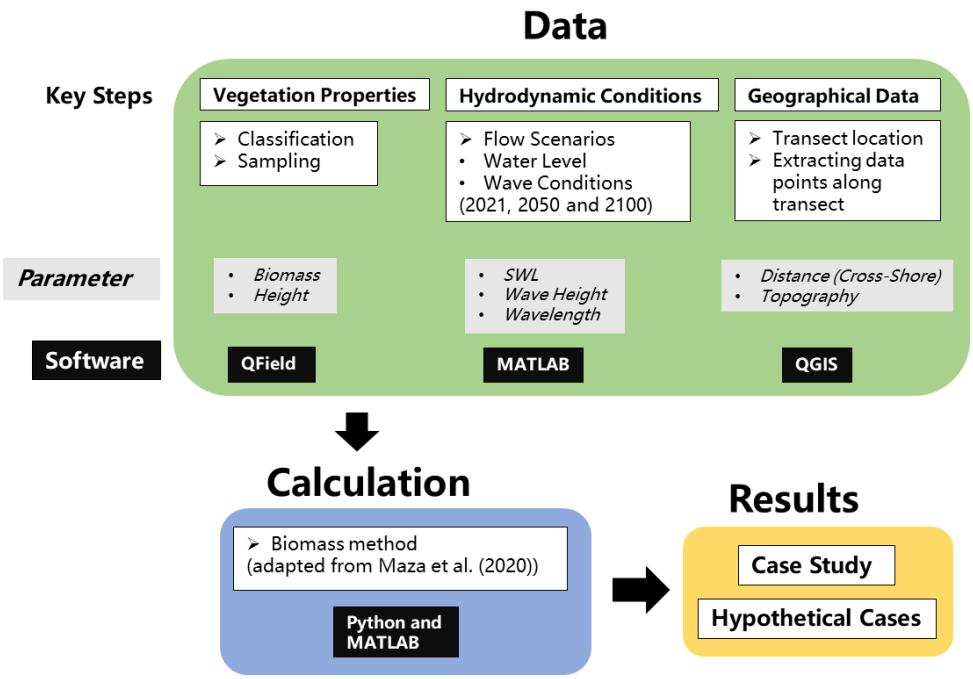

Figure 4. The work-process outlining the key steps and software used in each stage.

4.1 Classification of Vegetation

Vegetation height and biomass vary between plant species and more generally between plant communities. Since multiple different plant communities are present at Bunkeflo salt meadows, classification into different vegetation types is required. Maza (2020) suggested that vegetation height and biomass can be obtained by remote sensing or unmanned aerial vehicle (UAV) imagery (Doughty & Cavanaugh, 2019). However, depending on the application, resources and site characteristics, these methods may be impracticable. Remote sensing requires access to high-resolution images and UAV imagery requires expertise, drone sensors and likely calibration. For this study, classification by conducting field surveys was considered to be most effective. By visual inspection surveys of the study area, distinctly different types of vegetation were identified, with regards to the height, stem density and flexibility of the plants. The exact distinctions between the different vegetation types, for instance regarding vegetation height, or the number of classes, are somewhat arbitrary and represent the authors' views on the types of vegetation present.

To classify the area on site, the open-source mobile application QField (OPENGIS.ch, 2021) was used. By developing a project file in QGIS, the mobile application could be efficiently used to classify vegetation type boundaries. An aerial RGB image was used as a canvas to draw the vegetation types and was validated by on site observations. In cases where a vegetation class was only visible on site, its geographical extent was entered into QField using GPS coordinates obtained from the mobile phone.

Since the calculation method presented by Maza et al. (2020) relies on biomass and height as input parameters, the calculation method was not considered applicable to areas of very low vegetation biomass/height. This was also confirmed by mail correspondence with Maza (personal communication, April 9, 2021). In practice, this meant excluding large parts of the salt meadows that are used for grazing. In these parts, most vegetation had a height of only a few centimetres (~0-4 cm; vegetation type low meadow). However, in some areas of the grazed meadows slightly higher vegetation could be found (~4-13 cm; vegetation type high meadow). The biomass method was considered applicable to these small areas and samples were taken, but due to their spatial distribution they are not included in any of the final transect calculations. Other excluded parts of the study site were those that were forested or had large shrubs, bushes, and trees, since woody perennial vegetation is unsuitable for the biomass method (Ibid.) (Figure 5). Consequently, only four vegetation classes were considered suitable for application of the biomass method,

namely: high reed, low reed, high grass and high meadow. The classes high reed and low reed are almost exclusively dominated by *Phragmites australis*. On the other hand, the classes high grass and high meadow include a variety of different plant species. It has therefore not been possible to specify the dominating plant species within these two classes. In Figure 5 (below) the four different vegetation classes are shown.

Due to lack of time, the entire nature reserve of Bunkeflo salt meadows could not be classified. Classification was done between Lernacken in the north (excluding the western-most peninsula) down to about 200 m south of Strandhem.

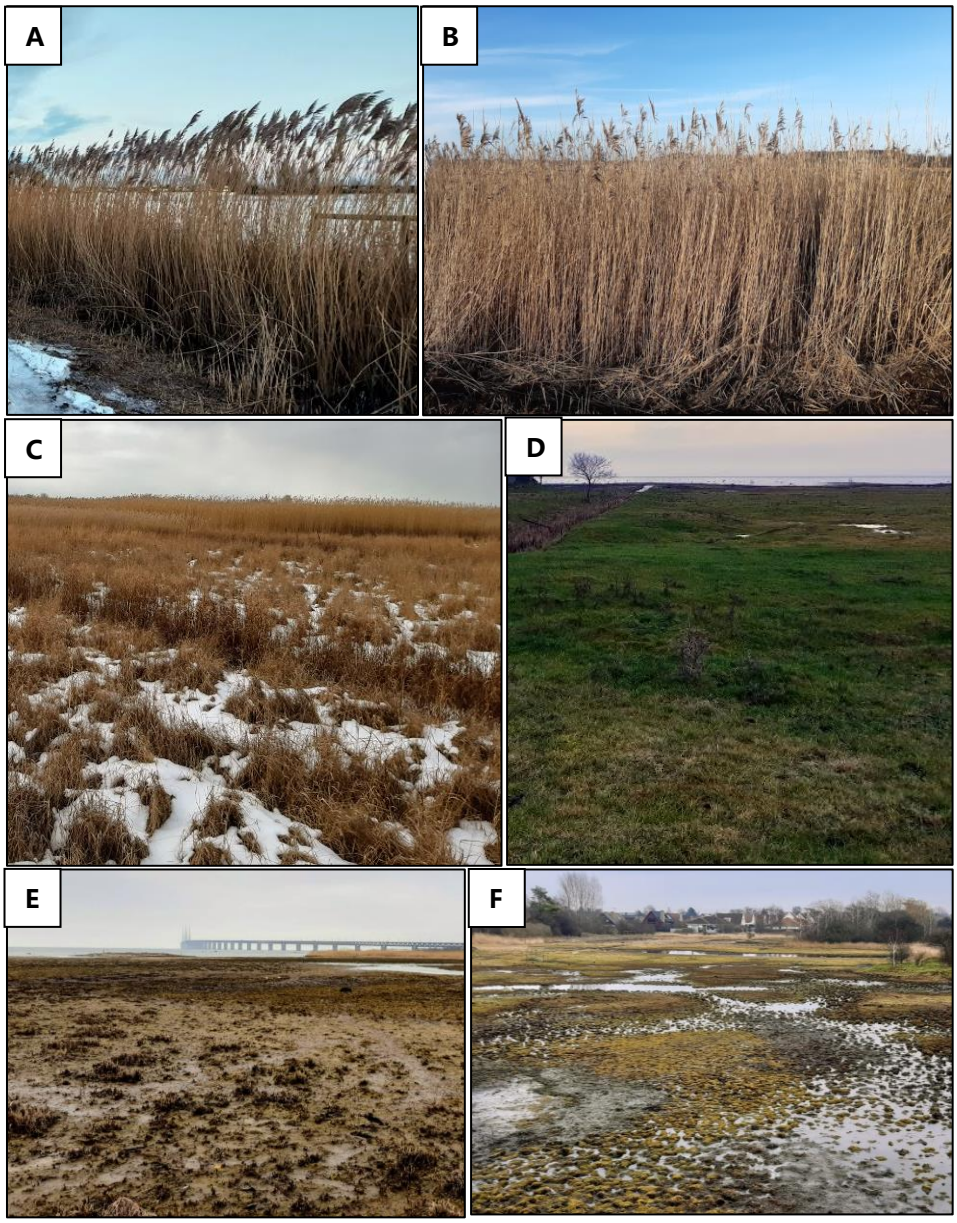

Figure 5. Variety of habitats found at Bunkeflo salt meadows. The four different vegetation classes included in the wave damping calculations are: high reed (A), low reed (B), high grass (C) and high meadow (D). Three excluded vegetation types are: mudflats (E) and low meadow and forest and bushes (F). The white areas in (C) are snow, and therefore parts of the vegetation are not visible.

4.2 Vegetation Sampling

The results of the classification of vegetation provided the basis for vegetation sampling. In each vegetation category, seven sampling points were randomly chosen. For a map of the location of the sampling points, see Appendix A3. The vegetation was sampled in late February when the vegetation was dormant, providing a low estimate of biomass. The biomass is likely to vary significantly between seasons, which is not considered in this thesis. The reasons for sampling the vegetation during winter are twofold. First, in southern Sweden storms are more frequent during this time of year. Hence the vegetation cover that was sampled was representative for the time of year that has the most storms. Second, if using calculations of wave damping from biomass for design purposes, it is recommended to assume a worst-case scenario and hence a low biomass to avoid overestimation.

At each sampling point, the height of the vegetation was measured before removing all standing vegetation from a square of 0.5 m x 0.5 m. This is method is known as destructive sampling. For more information, see Reinsch et al. (n.d.) After removing the above-ground biomass, it was dried. Due to lack of oven space, the samples could not be oven-dried in their entirety. Instead, the vegetation was first allowed to air dry in paper bags at room temperature for 7 days, before oven drying one subsample from each sample point. A laboratory oven was used at Sweco in Malmö. The oven was set at 70° C, and the biomass was dried for 24 hours. The weight after air drying and after oven drying was recorded so that a moisture ratio of oven-dried to air-dried biomass could be established. This ratio was then multiplied with the air-dried biomass of each sample to estimate the oven dried weight (see Appendix A3).

Mean values of biomass and vegetation height, along with 95 % confidence intervals, were then calculated. The mean values were used as input in further calculations. As a point of further analysis, biomass densities and vegetation submergence ratios for different water depths were also calculated. Density was calculated as kilogram dry weight per square meter divided by the vegetation height, while submergence ratio was calculated as defined in section 3.5.

4.3 Hypothetical Cases

The basis for the calculations differed between the case study and the hypothetical cases. For the hypothetical cases, a base scenario was chosen with the parameters defined according to Table 3 below. The choice of a 0.18 m incident wave, a period

of 4 s, 0.5 m water depth and 10 m transect length is based on a scenario used by Maza et al. (2020). The wavelength was calculated from the period and water depth according to linear wave theory. The choice of base case is essentially arbitrary. The hydrodynamic conditions used here were chosen for ease of comparison with results by Maza et al. (2020) whereas the vegetation type low reed was chosen because this vegetation type covers a large part of several of the studied transects. Unless otherwise stated, the values in Table 3 were used in the procedures explained below.

Table 3. Base case parameter values in the hypothetical cases.

Vegetation type	**h (m)**	**H_0 (m)**	**T (s)**	**L (m)**
Low Reed	0.5	0.18	4	8.67

Choosing low reed as base case, the wave damping after 10 m was plotted as a function of biomass, incident wave height, wavelength, water depth and vegetation height to see how each individual parameter affects wave propagation. When biomass was changed, the vegetation height was kept constant. This corresponds to a change in shoot density. However, when vegetation height was changed, the biomass was set to change accordingly to keep biomass density constant. For values of biomass, vegetation height and biomass density for low reed, see section 5.2.

To see how damping capacity differs between vegetation types, the relative wave height along a 10 m transect was plotted for the different types. This was done for four water depths; 0.25 m, 0.5 m, 1.0 m and 2.0 m. Additionally, the submergence ratio and its influence on wave damping after 10 m was compared between the different vegetation types. A sensitivity analysis was also performed to see how the original wave damping would change when the input parameters to the damping coefficient equation (Eq. (4)) were changed. The sensitivity analysis was performed on low reed and high grass to compare how parameters are influenced by the vegetation being emergent or submerged.

The calculations were performed in the calculation software MATLAB. For details on calculations and MATLAB scripts for the hypothetical cases, see Appendix A5.2.

4.4 Case Study

4.4.1 Inundation Scenarios

To define the water depth along transects and the incident wave height for each transect a combination of 100-year water levels and extreme wave heights were used. This section details which water levels were chosen. Section 3.5 explains how incident wave heights were calculated and which incident waves were chosen for the different scenarios.

The water depth at the shoreline was based on extreme water levels that have a return period of 100 years. This is shown in Table 4. The water levels are given in the height system RH 2000. It was assumed that the water level for the year 2021 is the same as the mean level in the period 1986 – 2005, which is probably an underestimation since sea level has risen since then. The water level for 2100 was taken from SMHI (2018) while the mean sea water level in the period 1986 – 2005 was taken from SMHI (2020). The 100-year level for 2050 was calculated according to the method outlined by SMHI (2020). For details, see Appendix A2. The 100-year water level relative to mean sea level in each scenario was assumed to be 1.41 m, in accordance with calculations by SMHI (2020).

Table 4. The 100-year water levels for different years, shown in RH 2000.

Year	Water level (RH 2000, m)
2021	1.53
2050	1.75
2100	2.17

4.4.2 Wave Transformations

As wind waves that are generated at sea move towards the shore, the changing water depth causes their wavelength and wave height to change in a process known as shoaling (USACE, 1984). If waves approach the coast at an angle they will refract, which further causes the wave height to change. Additionally, if wave heights are greater than a certain fraction of the water depth, they will break, which limits the wave maximum height. These calculations assume that bottom contour lines are straight and parallel. Figure 6 below shows the contour lines with 1 m interval, as

well as the 0.75 m and 0.5 m contour lines. Based on this figure, the assumption of straight and parallel contour lines was deemed reasonable.

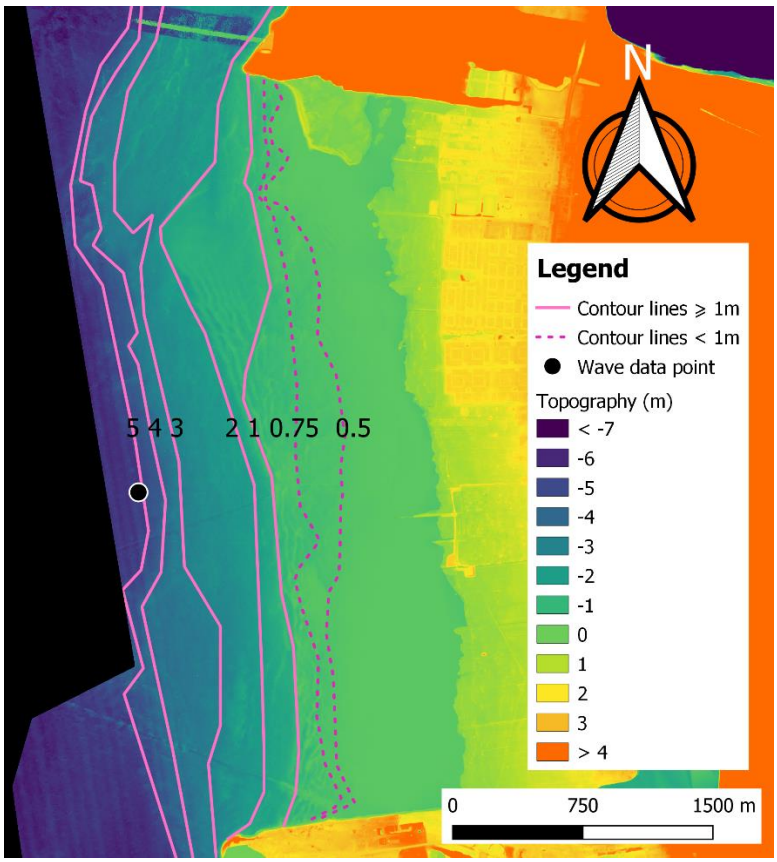

Figure 6. Topography and bathymetry (in RH2000) for Bunkeflostrand. The solid pink lines indicate the bottom contours with 1 m intervals, the dashed purple lines indicate 0.75 m and 0.5 m bottom contour lines. The point indicates the coordinates from which wave data was gathered. Black areas indicate that bathymetry data is not available. Map data from: Skåne Batymetri 1 m, © SGU, and Höjddata, Grid 2+ 2019, © Lantmäteriet.

To choose an appropriate incident wave height and wavelength as an input in the calculations, a 40-year time series of simulated wind waves was used. The data was generated using a SWAN model and was made available by Adell et al. (2021). It includes the wave height, significant period, and water depth of waves at a point approximately 1.5 km from the shoreline at Bunkeflostrand (black point in Figure 6).

In combination with the water levels associated with each scenario (section 4.4.1), a time series was obtained with wave heights, wavelengths, and the significant

period at the shoreline for each scenario. The location of the shoreline is assumed to be the same in all scenarios and is defined as the topographical line with an elevation of 12 cm in RH 2000. This corresponds to mean sea level in the period 1986-2005 at Bunkeflostrand (SMHI, 2020).

From this time series, the maximum wave height with the maximum wavelength was chosen as the incident wave in each scenario. In this way, each scenario combines a 100-year water level for that year with the maximum wave height and wavelength from the 40-year time series. This was done to represent a worst-case wave height scenario. Table 5 summarises the incident wave height and wavelength at the shoreline in each scenario.

Furthermore, it was assumed that linear wave theory applies and that waves break when the wave height is greater than 78 % of the water depth. For details about how wave transformations were calculated, see Appendix A5.2.

Table 5. Wave height H and wavelength L at the shoreline for each scenario. Values have been rounded off to 3 significant digits.

Scenario (year)	H (m)	L (m)
2021	1.10	24.9
2050	1.27	26.7
2100	1.60	29.8

4.4.3 Calculation Method

Once the study area was classified and the hydrodynamic scenarios defined, calculations were performed for four transects (Figure 8). Data points, containing vegetation height and biomass, topography and cross-shore distance, were generated in QGIS for every meter along the transects. Thereafter, the hydraulic biomass was calculated at each data point with Eq. (4). The incident wave height (H_i) used in Eq. (4) was updated every 10 meters. The update is required since the vegetation, water depth, wave height and length changes moving cross-shore. Furthermore, $L_{veg} = 1$ since the unit length of the transect is per meter.

To enable the use of Eq. (1) to calculate the wave damping, only one value of the damping coefficient can be inserted. If the damping coefficient changes, the equation cannot directly account for this. Therefore Eq. (1) was modified as follows:

$$H(x_n) = \frac{H_{0,n}}{1 + \beta_n x_n} \tag{7}$$

And:

$$H_{0,n} = H(x_{n-1}) * (1 + \beta_n x_{n-1}) \tag{8}$$

Furthermore, Eq. (3) by Maza et al. (2020) was considered to give unreasonably high damping coefficients when biomass was low. Therefore, it was decided to a adapt a new, non-linear fit to the data provided by Maza et al. (2020). The relation, based on hydraulic biomass, is shown below:

$$\beta = 0.0122 * HB^{0.6058} \tag{9}$$

A script was written in Python (Appendix A5.1) using Eq. (7) and (9). The information from the transect data points was exported from QGIS and run in the script for each point along the transect as illustrated in Figure 7. For motivation and details on the developed equations, see Appendix A1.

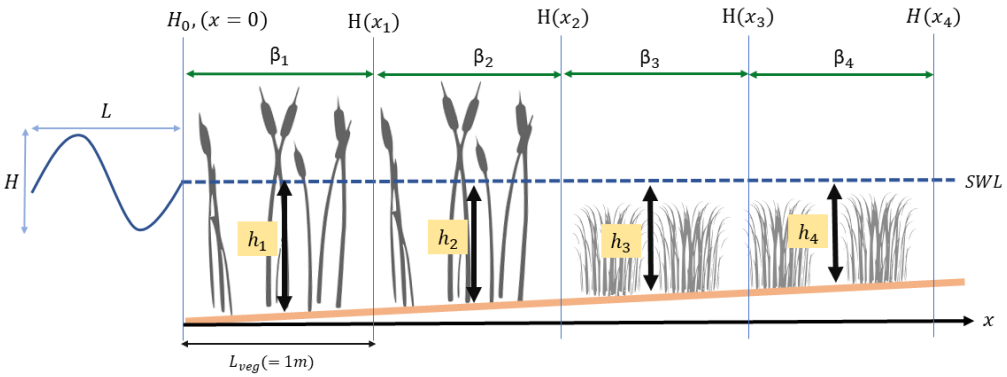

Figure 7. Schematization of the final calculation method.

5 Results

5.1 Classification of Vegetation

The result of the classification of vegetation is shown in Figure 8. Image A shows the northern part of the salt meadows while the middle part is shown in image B. Image B also shows the location of the transects used in the calculations. Transect 1 is the shortest and passes through low reed and high grass. Transect 2 is the longest and passes through the same vegetation types as transect 1. Transects 3 and 4 are of approximately equal length. Transect 3 passes through a wide belt of high reed and then ends in high grass, while transect 4 only passes through low reed. Large parts of the northern area are classified as low meadow, with small pockets of high meadow. None of the transects cross any of these vegetation types. The parts that are covered by forest and bushes are also not represented in any transect.

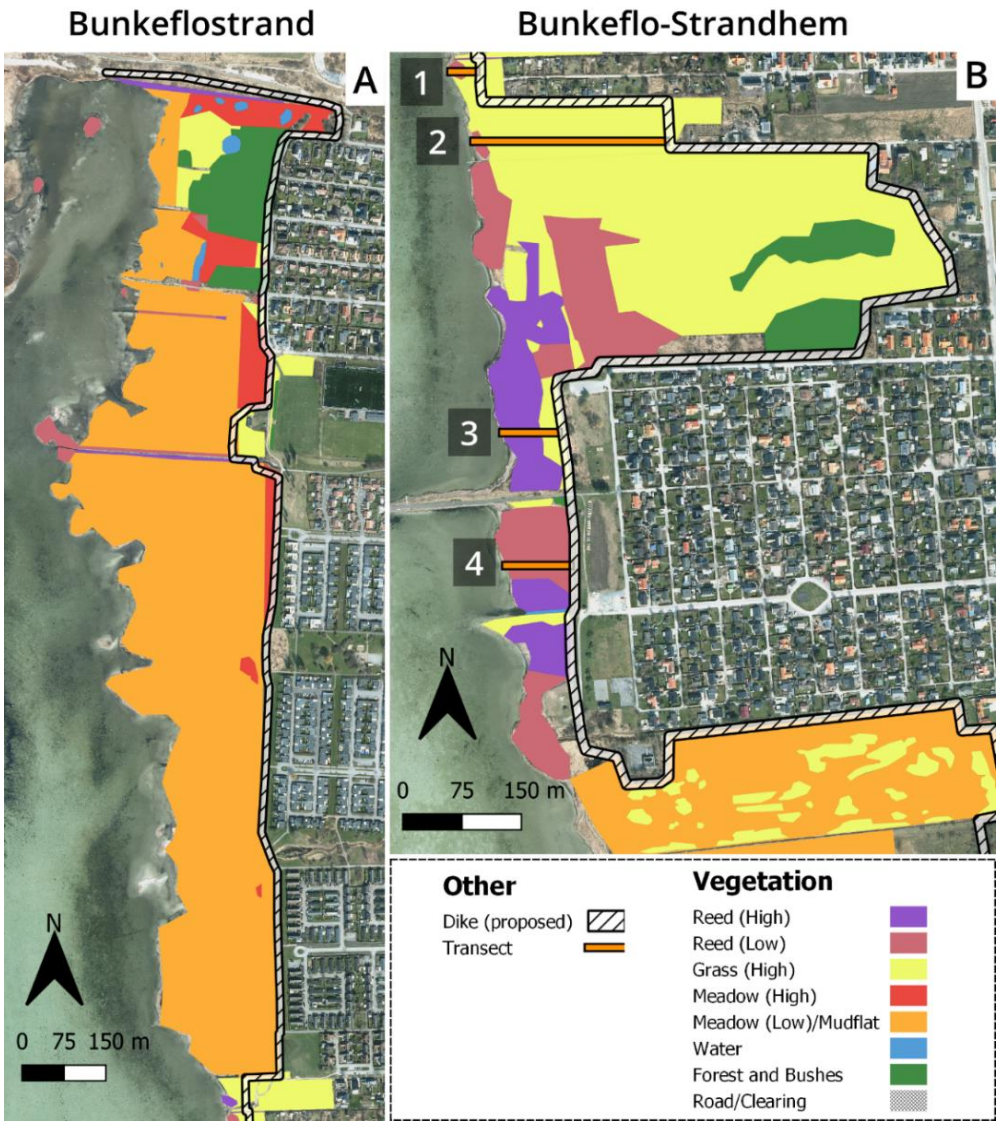

Figure 8. Classification of vegetation types from north (A) to south (B). Transects are depicted as orange lines, numbered from north to south. Map data (excluding dike location) from: Ortofoto RGB 0.25 m latest, © Lantmäteriet.

5.2 Vegetation Sampling

The above-ground dry biomass and vegetation height for each vegetation category is presented with a 95 % confidence interval in Table 6. For raw data, see Appendix A3. As can be seen in the table, the biomass confidence intervals of high reed and low reed overlap, whereas their vegetation heights do not. High grass and high meadow have clearly separated intervals of biomass and vegetation height.

Table 6. Above-ground dry biomass and vegetation height for the different vegetation types. The 95 % confidence interval (CI) is indicated in brackets. RH = high reed, RL = low reed, GH = high grass, MH = high meadow.

Vegetation	RH	RL	GH	MH
Biomass (kg/m^2) (95% CI)	**1.74** (1.09 – 2.39)	**1.27** (0.82 – 1.73)	**0.53** (0.37 – 0.69)	**0.14** (0.10 – 0.19)
Vegetation height (m) (95% CI)	**2.13** (1.89 – 2.36)	**1.58** (1.37 – 1.79)	**0.36** (0.27 – 0.45)	**0.09** (0.04 – 0.13)

A deeper investigation of the biomass and vegetation height is shown in Table 7 and Table 8 below. Table 7 shows that the density of low reed and high reed is very similar (0.81 versus 0.82 kg/m^3) whereas high grass and high meadow have very distinct densities (1.47 and 1.68 kg/m^3, respectively). The reed densities are also much lower than that of high grass and high meadow.

Table 7. Biomass density of different vegetation types. RH = high reed, RL = low reed, GH = high grass, MH = high meadow.

Vegetation	RH	RL	GH	MH
Density (kg/m^3)	0.81	0.82	1.47	1.68

Table 8 illustrates how the submergence ratio (SR) changes depending on water depth and vegetation type. The table shows three depths: 0.5, 1.0 and 1.5 m. Since the vegetation types have different heights, they will have different SR for different depths. For almost all depths in Table 8, low reed and high reed have SR = 1, except for 2 m water depth where SR for low reed is 0.79. For high grass and high meadow SR varies significantly, dropping to as low as 0.043 for high meadow in 2 m water depth. This is because reed is very tall compared to the grasses (for instance, 2.17 m for high reed vs 8.6 cm for high meadow).

Table 8. Submergence ratio in different water depths. If the vegetation height is greater than the water depth, SR = 1. RH = high reed, RL = low reed, GH = high grass, MH = high meadow.

Vegetation	RH	RL	GH	MH
h = 0.5 m	1	1	0.72	0.17
h = 1.0 m	1	1	0.36	0.086
h = 2.0 m	1	0.79	0.18	0.043

5.3 Hypothetical Cases

5.3.1 Influence of vegetation types

Figure 9 shows the relative wave height over a 10 m transect when covered with different vegetation types under four different depths. The results indicate that high reed and low reed generally reduce wave heights more effectively than high grass and high meadow (Figure 9 B, C and D). However, water depth plays an important role, with high grass showing higher damping than reed in very shallow water (Figure 9 A).

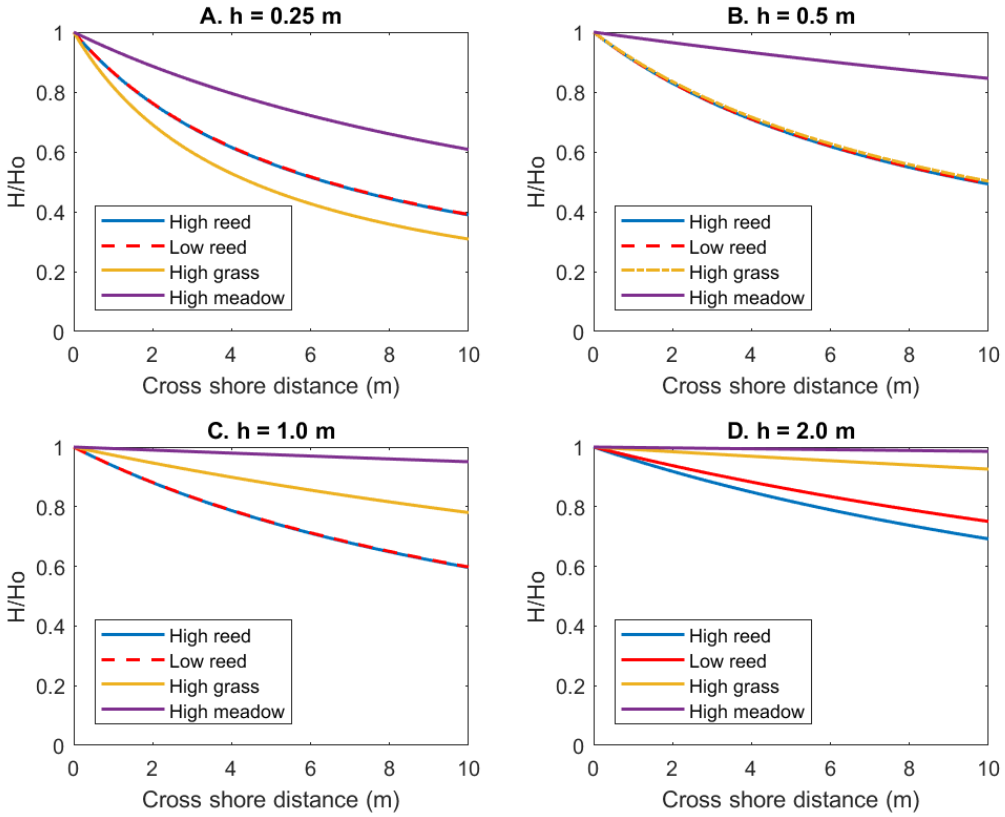

Figure 9. Wave damping from different vegetation types. High reed, low reed and high grass overlap. Water depth is A) 0.25 m, B) 0.5 m, C) 1.0 m, and D) 2.0 m.

The reason for these disparities is a combination of biomass density and submergence ratio. High grass has a higher biomass density than either high or low reed (Table 7). This causes a higher damping since a higher density, expressed as the biomass divided by the vegetation height, will increase the damping coefficient

(Eq. (4) and Eq. (5)). Additionally, for a given submergence ratio, high grass has a higher damping than high reed and low reed (Figure 10). Hence, when the water depth is only 25 cm, high grass has an SR of 1 and dampens waves with almost 70 %, compared to 60 % for high reed and low reed. However, in deeper water, high reed and low reed will have an SR greater than that of high grass (Table 8) and, consequently, have a greater damping. For instance, at 1 m water depth (Figure 9 C) high reed and low reed show a damping of 40 %, compared to only 22 % for high grass and 15 % for high meadow.

The combined effects of SR and biomass density also explains why high grass shows a damping similar to that of high reed and low reed when the water depth is 0.5 m (Figure 9 B). The high density of high grass compared to high and low reed roughly cancels out its lower SR, yielding a comparable damping of around 50 %. It also explains the relatively low damping of high meadow in all depths: although it has the highest biomass density, its low vegetation height (and hence low submergence ratio) causes the damping to be lower than the other vegetation types.

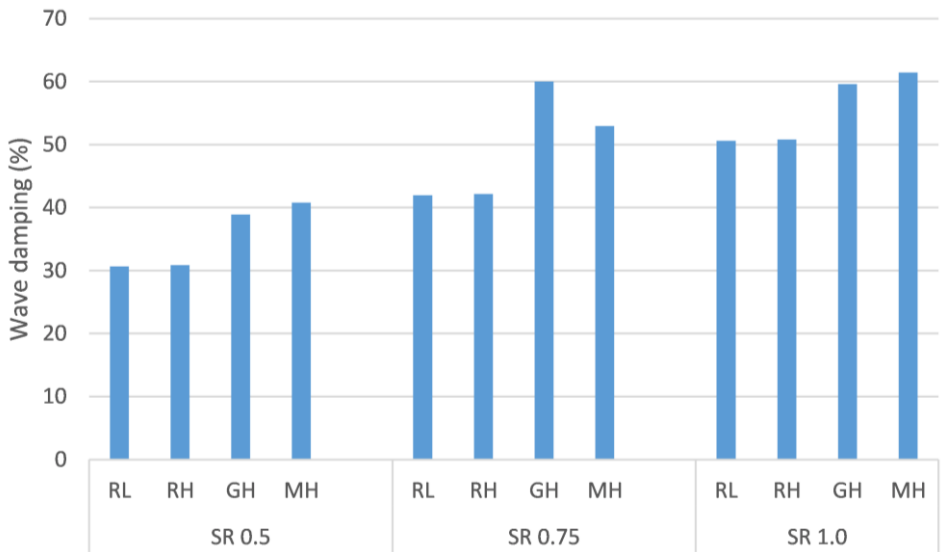

Figure 10. Wave damping as a function of submergence ratio (SR). RL = low reed, RH = high reed, GH = high grass, MH = high meadow.

These results can be compared to a study by Möller et al. (2011), who found that wave heights were reduced on average by 5.1 % per m in the transition zone from open water to reed, in reed beds in the southern Baltic. This translates to an average wave height reduction of 20.4 % over 4 m. The water depths in the exposed reed

bed in the study by Möller et al. (2011) ranged from 0.84 m to 1.56 m, with small waves, ranging from 0.8 cm to 27 cm. The hypothetical cases in this report are based on an incident wave height of 18 cm and water depths of 0.5 to 1.0 m. Hence wave heights, water depths and vegetation type are comparable to the study by Möller et al. (2011). In this report, wave damping by high reed and low reed at 4 m from the shoreline was approximately 30 % and 20 % for water depths of 0.5 and 1 m, respectively (Figure 9 B and C). This agrees well with the results by Möller et al. (2011) and suggests that the biomass method gives reasonable results for reed, at least in similar hydrodynamic conditions.

Regarding the classification of vegetation, it could be argued that high and low reed belong to the same vegetation type. The confidence intervals of their biomass overlap (Table 6), their biomass densities are very similar (Table 7), and they show practically the same damping except for in very deep water (Figure 9 D). The dominant species in both vegetation types is *Phragmites australis*, so the decision to split them into two categories may seem unwarranted. However, they do display distinctly different vegetation heights (Table 6). This has implications for wave damping when water when water levels are higher than the vegetation height. Since the decision to categorize the vegetation was motivated by the assumption that different vegetation types dampen waves differently, the high and low reed classes are valid, but mainly under extreme water levels.

5.3.2 Influence of different parameters

An analysis of the impact of various parameters is shown in Figure 11. The base line is a wave height of 0.18 m in 0.5 m water depth travelling over a 10 m transect covered by low reed.

Wave damping increases as biomass and incident wave height increase (Figure 11 A and B, respectively. However, the response is not linear, with a decreasing rate of change as biomass and wave height increase. Whether the wave damping tends towards a constant value is not possible to say in the intervals shown in Figure 11. Since the vegetation height was kept constant when changing the biomass, an increase in biomass can be interpreted as an increase in stem density. Several studies show an increase in damping with stem density (Augustin et al., 2009; Garzon et al., 2019) and biomass density (Bouma et al., 2010; Maza et al., 2015). Hence this result seems reasonable. As for incident wave heights, studies have shown conflicting results (see section 3.2). Maza et al. (2015) suggest that this may be related to differences in plant flexibility. When wave heights are low, increasing them may increase drag on stiff stems, causing more damping. When wave heights are very high, increasing them further may simply cause stems to fold, as observed

by Rupprecht et al. (2017). As the biomass method does not consider plant flexibility, it is difficult to evaluate whether higher damping is a plausible effect under the given plant conditions. This is related to wave energy conditions, which will be discussed in more detail in section 6.1.1.

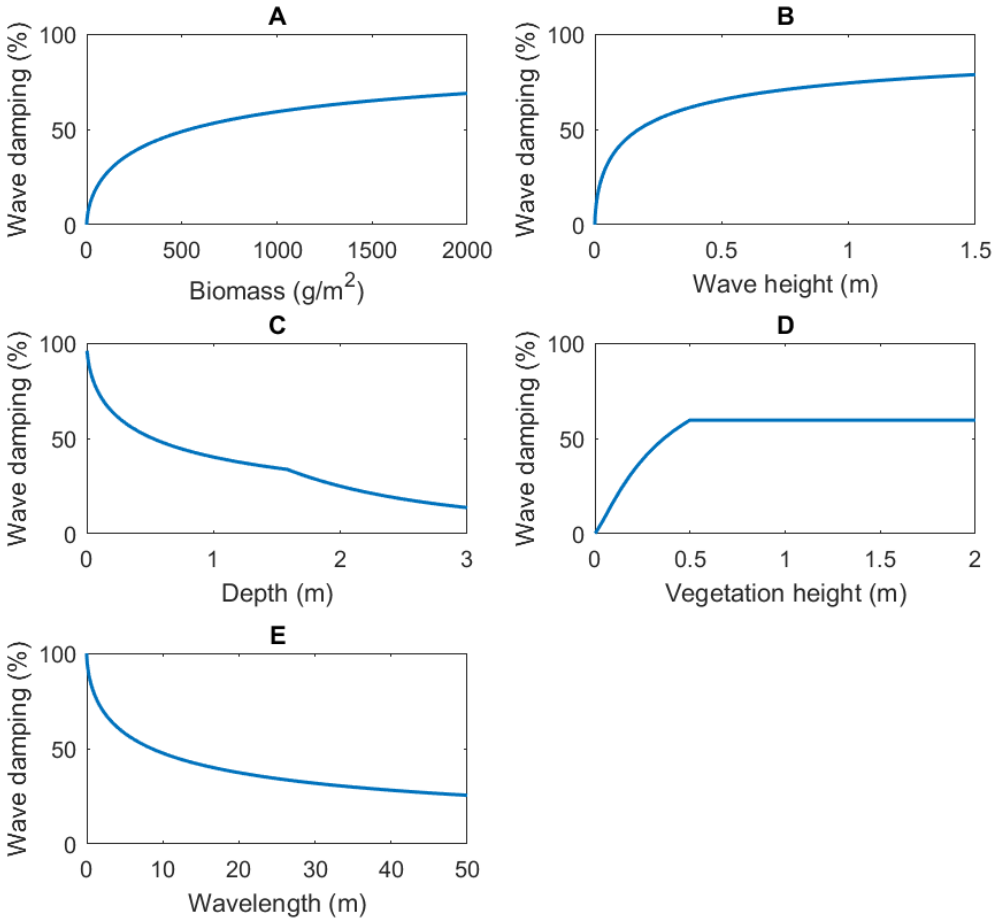

Figure 11. Wave damping as a function of A) Biomass, B) Incident wave height, C) Water depth, D) Vegetation height, and E) Wavelength. When damping is plotted as a function of vegetation height, the vegetation density is kept constant.

According to the results, wave damping decreases as water depth increases (Figure 11 C). There is a discontinuity in the curve at 1.58 m depth, after which the decrease in wave damping changes faster than in shallower water. This is the point at which the vegetation becomes submerged, and the submergence ratio becomes less than 1. Hence the damping coefficient will decrease, explaining the discontinuity.

Similarly, there is a discontinuity in the response of wave damping to changes in vegetation height (Figure 11 D). As vegetation height increases, damping also increases until the vegetation height is 0.5 m, after which the submergence ratio becomes 1 and the wave damping becomes constant at approximately 50 %. In Figure 11 D, the vegetation density has been kept constant so that, when the vegetation height changes, mass varies accordingly. Hence, after SR = 1, any change in vegetation height is cancelled out by a corresponding change in biomass, meaning the wave damping stays constant. In summary, the relationship between the vegetation height and the water depth is very important for wave damping, according to the biomass method.

The results also show that an increase in wavelength decreases the wave damping (Figure 11 E). Like other parameters, the damping is non-linear, asymptotically approaching a damping of around 25 %. The non-linear response is a consequence of the new β-relation, which is an exponential relationship.

5.3.3 Sensitivity analysis

The sensitivity analysis shows that the impact of water depth and vegetation height are much more pronounced when the vegetation is submerged than when it is emergent (i.e., when $h_{veg} < h$). Figure 12 illustrates the percentage change in wave damping when a certain parameter is either 50 %, 100 % or 200 % of its base case value. Two vegetation types (low reed and high grass) are shown to illustrate the effect of $h_{veg} < h$ and $h_{veg} > h$. Note that although the absolute wave damping may be different, all parameters behave the same for low reed and high grass, with the notable exception of h_{veg} and h. Since the reed is so high, its SR is 1, so changing the vegetation height does not cause a change in wave damping. For the grass, the vegetation height does play a significant role since increasing it will increase SR and hence the wave damping. As for water depth, it behaves the same as the other parameters for low reed, i.e. when SR = 1. However, for high grass it is a much more sensitive parameter, causing higher damping when it is halved and much lower damping when it is doubled compared to all the other parameters.

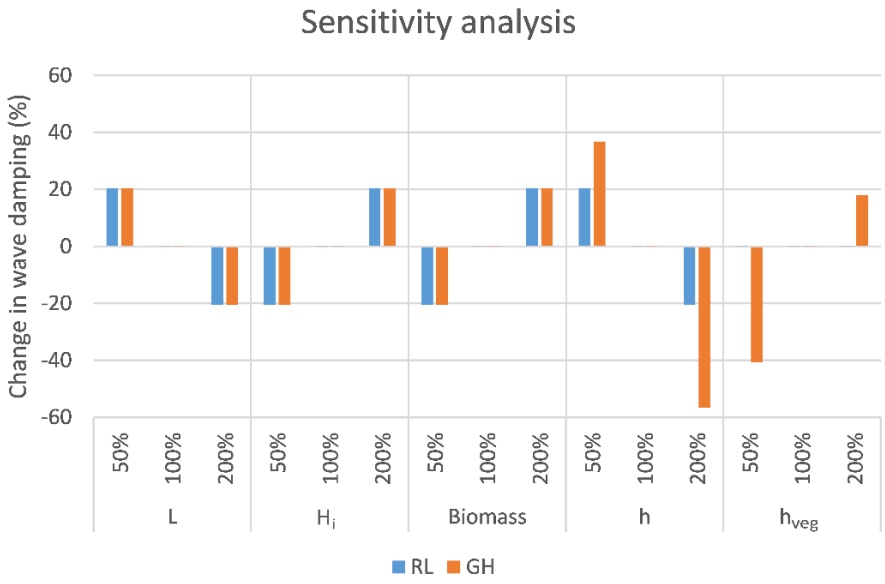

Figure 12. Sensitivity analysis of parameters used in the biomass method, illustrated with RL (blue) and GH (orange).

As outlined in section 3.2, several studies have shown the importance of water depth to wave damping. For instance, Garzon et al. (2019) found that water depth relative to vegetation height plays an important role. However, they also noted that certain parameters (such as stem density and diameter) had a different correlation with wave damping depending on whether the vegetation was submerged or emergent. This would suggest a discontinuity in wave damping as vegetation transitions from being submerged to emergent, which agrees with the transition points in Figure 11. The results in Figure 11 also agree with previous studies that wave damping decreases with increasing water depth and decreasing vegetation height, which again explains the higher damping by reed compared to the other vegetation types.

The sensitivity analysis shows that for the emergent reed, the damping is unaffected by vegetation height since the water depth is so low (0.5 m). Therefore, even if the height of the reed is reduced by 50 % the reed canopy will still be above the water level (Figure 12). However, this contradicts results by Möller et al. (2011) who studied reed beds in the Baltic Sea. Although the reed was never submerged in that study, they still found a strong dependence of wave damping on water depth. They attributed this either to lower friction from bottom shoots or to greater swaying of the reed stems when water depths increased. This indicates a limitation of using biomass as a proxy, as it leaves out such biomechanical properties of the plant species.

5.3.4 Mathematical analysis

When discussing the influence of relative water depth in the biomass method, it is helpful to study the damping coefficient to see what happens when the vegetation is emergent or submerged. Recall that hydraulic biomass (Eq. (4)) is calculated as:

$$HB = \frac{W_{dry}}{h_{veg}} * min(h_{veg}, h) * SR * \frac{L_{veg}}{L} * \frac{H_i}{h} \tag{10}$$

In this thesis, a new relationship between β and HB has been used as was shown in Eq. (9). This means that, for different relations between water depth and vegetation height, the damping coefficient reduces to the following:

$$\beta = \begin{cases} a * \left(\frac{W_{dry}}{h_{veg}} * \frac{L_{veg}}{L} * \frac{H_i}{h}\right)^b, & h_{veg} \geq h \\ a * \left(W_{dry} * h_{veg} * \frac{L_{veg}}{L} * \frac{H_i}{h^3}\right)^b, & h_{veg} < h \end{cases} \tag{11}$$

To simplify readability of the equation, the coefficients in Eq. (9) have been replaced here with a (=0.0122) and b (=0.6058). By studying the equations above it becomes apparent why all parameters, except water depth and vegetation height, in the sensitivity analysis influence the wave damping in the same way when lowered by 50 % or increased by 200 % (Figure 12). Doubling biomass in the equation will be mathematically equivalent to doubling the incident wave height. It also shows why the water depth has such a large influence on the wave damping under submerged conditions, as β is a function of h^3 when the vegetation is submerged. This points to an important fact, which is that the results in this thesis reflect how the biomass method responds to different hydrodynamic conditions and vegetation characteristics. They do not necessarily reflect how wave damping would in fact be influenced by changing the parameters in real conditions. To make sure that the model accurately reflects different situations it would need to be validated, especially for the high wave energy conditions explored in this thesis.

5.4 Case Study

The changes in wave heights along the four transects at Bunkeflo salt meadows are shown in Figure 13. For all transects, the 100-year inundation level in the year 2100 has the highest wave height at the end of each transect. Longer transects seem to result in smaller final wave heights, especially when comparing the shortest (transect 1, 32 m) with the longest (transect 2, 232 m). This is to be expected since Eq (1) will inevitably lead to a lower relative wave height as the cross-shore distance increases. A review by Shepard et al. (2011) found that wave damping was positively correlated with the length of the vegetation field in all the reviewed studies. Hence this result has strong support in the literature.

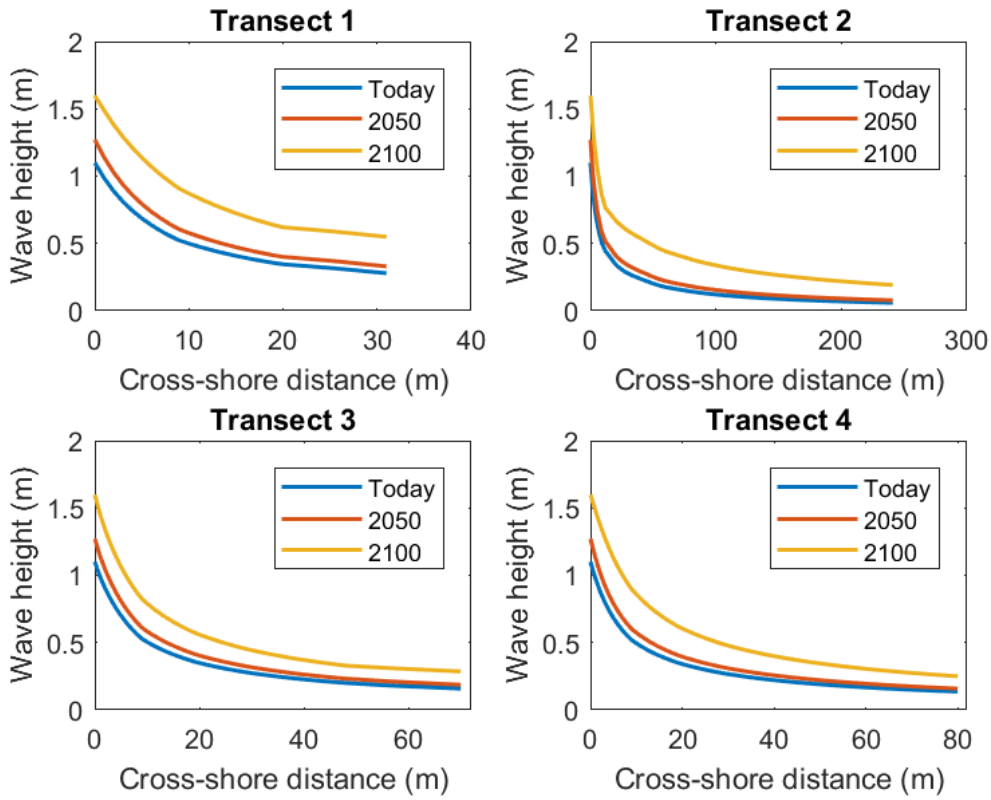

Figure 13. Wave damping along the transects for each scenario. The results assume water levels corresponding to the 100-year inundation level for each year.

Table 9 summarizes the results by showing the absolute wave height and the percentage wave damping at the end of each transect in each scenario. This table illustrates that longer transects result in more wave damping than shorter ones: For the year 2021, the longest transect (transect 2) shows a maximum wave height

reduction of 94.6 % compared to the shortest (transect 1) which has a reduction of 74.6 %. In rising order, transect 3 (70 m) has 85.6 % damping and transect 4 (80 m) has 87.6 % damping for the year 2021. The lowest wave damping occurs in the year 2100 in transect 1, in other words in the shortest transect during the scenario with the deepest water and largest wave heights. In this case the damping is 65.6 %. The largest total damping occurs in transect 2 in the year 2021, with 94.6 % damping. This is the longest transect in the scenario with most shallow water and smallest incident wave heights.

Table 9. Wave heights at the end of each transect and corresponding wave height reduction in percent. The latter is marked in bold text.

Transect / Year	1		2		3		4	
	H (m)	**Damping (%)**	H (m)	**Damping (%)**	H (m)	**Damping (%)**	H (m)	**Damping (%)**
2021	0.279	**74.6**	0.059	**94.6**	0.158	**85.6**	0.136	**87.6**
2050	0.330	**71.6**	0.078	**92.0**	0.187	**83.9**	0.158	**86.6**
2100	0.549	**65.6**	0.192	**88.0**	0.286	**82.1**	0.250	**84.4**

In general, the results indicate that the meadows are of great importance to coastal protection, especially at areas such as Strandhem, which are close to the shore and hence are more exposed to wave action. At Strandhem, wave heights were reduced by between 82.1 % and 87.6 %, depending on scenario and transect (Table 9). When comparing transects to each other, wave heights at similar distances from the shoreline are lower in transects 3 and 4 than in transects 1 and 2 (Figure 14, Figure 15). The results from the classification (Figure 8) show that the vegetation along transects 3 and 4, which are located at Strandhem, is mostly composed of either high or low reed. This explains the higher damping over those transects compared to similar distances in transects 1 and 2, since according to the hypothetical cases (Figure 9), high and low reed are more effective at damping waves compared to high grass and high meadow, except in very shallow water.

It is also interesting to note that under lower water levels, such as in the 2021 scenario, the difference between transects is small. This again shows how the damping capacity of high grass, according to the biomass method, is comparable to that of reed under low water levels, as was discussed in section 5.3.1.

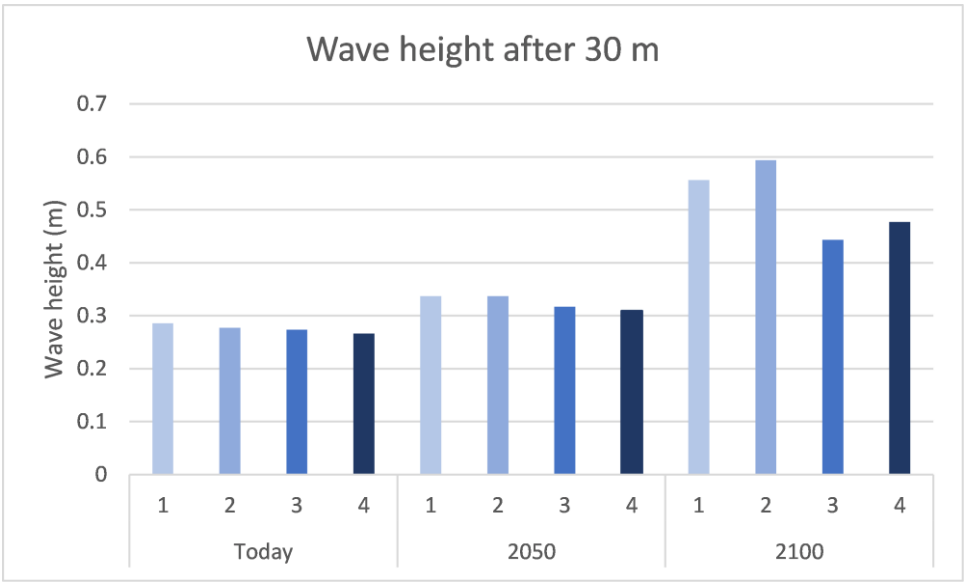

Figure 14. Wave height 30 m landwards from the shoreline for each transect and respective scenario.

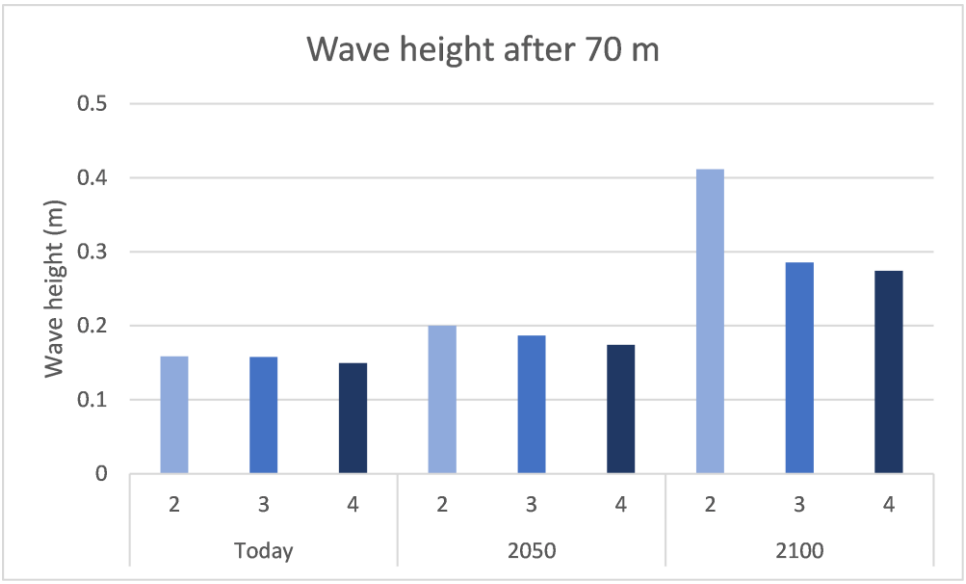

Figure 15. Wave height 70 m landwards from the shoreline for transects 2, 3 and 4, for each scenario. Transect 1 is omitted since its total length is less than 70 m.

5.5 Comparison with other studies

Since many different factors influence wave damping, it can be difficult to compare the results of different studies. However, it is still valuable to see how total damping over transects in field studies compare to the results for the transects at Bunkeflostrand. In the Chesapeake Bay on the U.S. east coast, Garzon et al. (2019) found that wave heights of 1.55 m could be damped by 50 % over 250 m. In comparison, this report shows an 88 % reduction of a 1.6 m wave over 232 m (Table 9). In other words, a significantly greater damping happened over a slightly shorter distance. A possible explanation is that the 1.55 m wave reported by Garzon et al. (2019) was associated with a much greater water depth of 4.5 m, compared to 2.2 m at the shoreline in this report (Table 4). As was discussed in section 5.1, a greater depth seems to cause a reduction in wave damping, which indicates that the damping over long transects in this report is large but not implausible.

Möller et al. (1999) saw, on average, a 61 % wave height reduction over 180 m in a saltmarsh on the eastern coast of the U.K. Significant wave heights ranged from approximately 0.3 m to almost 0.7 m. Water depths varied between 0.53 and 1.39 m. Since measurements were made during spring tide, it meant that the vegetation was submerged, with the canopy ranging from 0.12 m to 1 m below the surface. This can be compared with a 65.6 % reduction over transect 1 (30 m) in the year 2100 (Table 9). Hence a much shorter distance still shows a slightly larger wave damping. Again, the explanation might be found in the water depth. In transect 1, the first 20 m consists of high reed (Figure 8) which is emergent in all scenarios, compared to the submerged vegetation in the tidal saltmarsh. According to the previous discussion on relative water depth, higher damping is to be expected when the vegetation is emergent compared to when it is submerged. However, wave heights in this report are significantly greater than in the study by Möller et al. (1999), possibly making comparisons misleading. Whether or not higher incident wave heights could be expected to cause more damping or less will be discussed in section 5.3. Additionally, 180 m is quite a long transect, so a comparable damping over 30 m indicates an overestimation of the wave damping by the biomass method.

From the studies above, the results from the transects studied in this thesis may be plausible but tend towards overestimation. However, since many factors affect the results, it is difficult to compare the findings from one study directly to another. To overcome this issue, data from Bouma et al. (2010) and Möller et al. (2014) were used in the biomass method to calculate wave damping. Table 10 and Table 11 compare the reported wave damping from these studies with the wave

damping calculated using the biomass method. Bouma et al. (2010) studied wave damping by two species, *Spartina anglica* and *Puccinellia maritima*, whereas Möller et al. (2014) studied damping from a section of saltmarsh dominated by the species *Elymus athericus*.

The biomass method applied to data from Bouma et al. (2010) overestimates the wave damping by 39.2 % on average (Table 10), whereas the overestimation for the study by Möller et al. (2014) was 27.5 %, on average (Table 11). Since the biomass method considers hydrodynamic conditions such as water depth, vegetation height, and incident wave height, similar results should be attained. The fact that reported wave damping in flume studies is overestimated by the biomass method indicates that the method may be unreliable for estimating wave damping, despite plausible results over long transects.

Table 10. Wave damping reported by Bouma et al. (2010) compared to the wave damping calculated when inserting data from Bouma et al. (2010) into the biomass method. For details, see Appendix A4.

Bouma et al. (2010)	H_o (cm)	Damping, reported (%)	Damping, biomass method (%)	Difference (percentage units)
Spartina anglica	6.5	63.8	90.7	26.9
	6.7	49.1	88.3	39.2
	7.0	34.6	84.5	49.9
Puccinellia maritima	6.6	64.9	87.9	23.0
	6.7	39.2	83.1	43.8
	6.8	27.0	79.2	52.2
Average	-	-	-	**39.2**

Table 11. Wave damping reported by Möller et al. (2014) compared to the wave damping calculated when inserting data from Möller et al. (2014) into the biomass method. For details, see Appendix A4.

Möller et al. (2014)	H_o (cm)	Damping, reported (%)	Damping, biomass method (%)	Difference (percentage units)
Mixed canopy, dominated by *Elymus athericus*	10	0.0	38.4	38.4
	30	19.5	34.1	14.6
	60	13.8	44.1	30.3
	70	16.9	40.4	23.5
	90	16.9	47.8	30.9
Average	-	-	-	**27.5**

6 Discussion

6.1 Model Limitations

6.1.1 Wave Energy

Many laboratory and field studies have only tested and validated their results for low energy wave conditions. This is also true for the study by Maza et al. (2020). As mentioned in section 3.5, wave heights in the flume study by Maza et al. (2020) range from 0.08-0.18 m and the maximum depth is 0.4 m. In contrast, the scenarios in this thesis have wave heights ranging from 1.1 m to 1.6 m and water depths up to 2.05 m relative to mean sea level. Hence an empirical relationship validated for rather low energy conditions has been used to calculate damping in high energy wave conditions. Although the biomass method (Eq. (4)) does consider the wave conditions, it does not take higher wave energy into account and may therefore be inaccurate, which has been suggested in section 5.3.2. Higher wave heights indicate higher wave orbital velocities, which may induce a greater degree of swaying in the vegetation. The impact this will have on wave damping depends in part on the flexibility of the plant stems, which will be discussed in the following section.

6.1.2 Flexibility

As has been mentioned in section 3.2, several studies have indicated flexibility to be an important parameter for wave damping. The vegetation types high grass and high meadow consist of rather flexible vegetation whereas high reed and low reed are stiff. The biomass method does not take these variations into account, although other studies have attempted to quantify its importance. van Veelen et al. (2020) saw 70 % greater wave attenuation for rigid mimics compared to flexible ones, and attributed this to differences in drag force generated, where rigid vegetation causes higher drag forces compared to flexible mimics. Bouma et al. (2010) found that two species of very different flexibility still had similar wave damping capacity when expressed as a function of biomass. However, this may fail to account for differences in wave energy. For instance, Rupprecht et al. (2017) saw higher drag on rigid vegetation, indicating higher damping, but also noted that under high energy conditions, plants are susceptible to folding and bending, and stiff vegetation may even break, precisely due to low flexibility. Under storm conditions, especially during a long-lasting storm, it is then possible that the protective effect of stiff vegetation such as reed may decrease over time as more stems break. This highlights that although the results in this thesis indicate increasing wave damping

when incident wave heights increase, that may not be the case. Additionally, it points to the difficulties involved in modelling the effects of wave conditions affecting plant species with differing biomechanical properties, and that these properties may change when wave conditions change.

6.1.3 Other Hydrodynamic Factors

The calculation method used in this thesis is simple regarding the in- and output of hydrodynamic parameters. All that is required as input is wave height, wavelength, and the depth. However, what the method gains in simplicity it may lose in accuracy and detail. As mentioned previously, Mendez & Losada (2004) further developed Eq. (1) to take shoaling and breaking into account. They also developed Eq. (1) and validated the new equations for both nonbreaking and breaking random waves. Recently, Losada et al. (2016) extended the equations even further to include the effects of currents. Since all these advancements have been made in relation to a bulk drag coefficient and not the hydraulic biomass, they have not been possible to implement in this thesis. Additionally, Eq. (1) was developed for regular waves, whereas the significant wave height has been used as input in this report. Further developments are thus required to take random waves into account, especially since waves in nature are random and not regular.

Other effects, such as wave-setup and wind waves generated over the salt meadows have also been left out. Especially wind waves may be important to consider since the cross-shore distance of the meadow is often long. In summary, several important factors are omitted in the model used in this thesis. Among these factors, shoaling is probably the most important one in explaining the overestimation of wave damping since shoaling causes wave heights to increase as waves move landward. To include the effects of shoaling, more laboratory experiments would need to be conducted where the depth varies.

6.1.4 Biogeomorphic Variability

Beyond the direct interactions between plants and waves, there are other important in-direct effects that should be considered. As can observed at Bunkeflostrand, vegetation can cause increased spatial variability in the terrain, i.e. biogeomorphic variability. Figure 16 shows how vegetation can grow in patches and cause the formation of non-vegetated open water channels. A recent study by Yang & Irish (2018) investigated how wave damping is affected by the spatial variability in mound-channel wetland systems. They note that depending on wave frequency and location, the added spatial variability of patchy vegetation can, but does not always, decrease wave energy and hence wave height. Under certain conditions, Bouma et al. (2009) and Balke et al. (2012) observed that vegetation grouped in

patches also can increase plant growth rate and sediment accretion. This is a consequence of the positive feedback-loop caused by attenuated wave energy between the mounds.

Figure 16. Patchiness and open water channels at Bunkeflo salt meadows.

6.1.5 Linear versus Exponential β-fit

According to Maza et al. (2020), the relation between the damping coefficient and the hydraulic biomass is linear on the form y = kx + m. When the results in this thesis were examined, it was found that the constant term m = 0.1 (Eq. (3)) became highly dominant when calculating the damping coefficient, especially when biomass values were low. In many cases, the influence of hydraulic biomass was so small in comparison that it did not significantly affect the results. Since the term also implies that the damping coefficient is 0.1 even if there is no biomass, it was decided to create a new fit to the data presented by Maza et al. (2020). An exponential function was fitted, so that the damping coefficient is 0 when biomass is 0 (see Eq. (9)). This implies a constant wave height along transects if there is no biomass, which ignores processes such as shoaling and bottom friction not caused by vegetation. These limitations to the model have been discussed elsewhere (see sections 6.1.3 and 6.1.4).

The resulting fit showed a higher coefficient of determination (R^2=0.86) than the one presented by Maza et al. (2020). The new fit also resulted in more conservative values of the damping coefficient, which provided further justification for its use. A comparison between the two relationships (Eq. (3) and Eq. (9)) is given in Appendix A1 (Figure 19).

6.2 Model Applicability

Despite several extensions (section 6.1) that could be made to make the calculation method more accurate, the concept of using biomass as a proxy for the bulk drag coefficient does have a major advantage if the method does not require calibration. The bulk drag coefficient depends on the hydrodynamic conditions and the specific plant species characteristics and therefore it may take many years before there is enough data to make it reasonable to directly use literature values for C_d without calibration. Meanwhile, if calibration is required, many coastal projects may overlook the potential benefits of wave damping from vegetation if there is no simple way to quantify the benefits without calibration. On the other hand, dry weight biomass is a relatively well-known characteristic for many plant species and therefore may be easier to find data for in the literature (e.g. Feagin et al., 2011). However, even though the input parameters may not require calibration, the relation between them may. In this thesis, the relation between the damping coefficient and hydraulic biomass in Eq. (3) was replaced by Eq. (9), suggesting that the biomass model may need to be calibrated further. The comparison with other studies (section 5.5) also serves as a form of validation, and also suggests that calibration may be required, especially for high energy wave conditions. It is the opinion of the authors of this thesis that more research should be conducted to validate the method for storm surge conditions and for more plant species. If this is done, the biomass for a variety of plant species could be summarised in a chart, ready for direct implementation according to a calculation methodology similar to the one in this thesis.

Regardless of calibration and validation, wave damping results are probabilistic rather than deterministic due to aleatory and epistemic uncertainty. Due to the limited scope of this thesis, wave damping results are only presented as single values for each scenario. To improve the model and the reliability of the results, Monte Carlo simulations could be made. Thereby, the results would better account for the randomness of waves and other variability of the model parameters. This is especially important for risk assessments if vegetation fields are intended for use as coastal protection.

An advantage of the methodology developed in this thesis is that the cost of software and field equipment is minimal. Regarding software, the code in Python, QGIS and QField are all open-source and free to run. MATLAB is the only software that is not free, but all calculations that were made in MATLAB could have been performed equally well in Python. Regarding field equipment, all that was required was a smartphone to run QField, secateurs for cutting biomass, a ruler and a

wooden frame to measure the sample point area. To calculate the dry weight of the biomass it is advantageous to have access to an oven, but it is not necessarily a requirement since the biomass can also be air-dried.

A major limitation of using the calculation method based on biomass is that some areas (i.e. low meadow and mudflats) do not have wave attenuation from vegetation biomass since they have little or none. Similarly, wave damping calculations over areas with high and unevenly distributed biomass (i.e. forest and bushes) may also be misleading, but for the contrasting reason of having very high biomass. This is problematic since these vegetation types cover large areas of the study site. According to email correspondence with Maria Maza (personal communication, April 9, 2021) it may be more suitable to use other methods for these areas, such as an enhanced bottom friction factor. Therefore, to create a realistic model of the wave damping applicable to the entire area, it may be necessary to use multiple calculation methods, even along the same individual transects. However, this does complicate the calculation procedure. Therefore, the issue was avoided by simply excluding the areas of the salt marshes where these uncertainties arise.

Even though the wave damping of the low biomass areas cannot be quantified with the applied calculation method, previous studies give an indication of what wave damping can be expected from similar areas. Yang et al. (2008) analysed wave damping along a 185 m long unvegetated mudflat transect and showed a final wave height reduction of 11 %. Later, at the same site, Ysebaert et al. (2011) conducted wave height measurements across vegetated transects, suggesting the average damping in comparison to the mudflats was 20–50 times higher. Similar observations were made by Möller et al. (1999), concluding that wave damping over sand flats was significantly lower (on average 29 % damping) than over vegetated saltmarshes (on average 82 % damping). This is attributed to the greater surface friction of vegetated saltmarshes compared to unvegetated sand flats. Assuming that the physical characteristics of plants (e.g., vegetation height, biomass and flexibility) are the most important wave damping parameters, it is reasonable to expect wave damping is also less over grazed low meadows. Likewise, it is reasonable to expect the wave damping over forested areas to be high due to the high biomass, vegetation height and low flexibility.

6.3 Scenarios

In this report, the scenarios are based on the combination of a 100-year water level with extremely high wind waves. In reality, a situation with an extremely high water

level rarely coincides with large wave heights at Bunkeflostrand (Almström et al., 2017). This has to do with the hydrodynamic situation around the Limhamn shelf (SMHI, 2018). However, since the purpose of this thesis is to show the wave damping effect of vegetation, rather than to estimate actual wave heights at a given event, the combination of high water levels with large wave heights was found to be illustrative.

The three scenarios presented in Table 4 assume that the shoreline remains at its current position and that the vegetation of the salt meadow ecosystem remains unchanged. In other words, the scenarios are cases of extreme water depth without any change of the coastal habitat. However, it is likely that the effects of climate change, especially sea level rise, will cause both the shoreline and the vegetation to migrate. Furthermore, anthropogenic change, such as the introduction of a dike or a change in grazing areas, may also alter the vegetation on site. If the vegetation changes, it is also possible that sedimentation fluxes change and consequently also the geomorphology and topography. Therefore, it is important to emphasize that the wave damping in future scenarios may have changed considerably. It is consequently relevant to further investigate how the salt meadows are likely to respond to climate change, which is discussed in section 6.4 (below).

6.4 Implications for Coastal Protection and Climate Change Adaptation

Considering that the wave damping from vegetation is a climate change adaptation strategy, it is fundamental to understand whether the salt meadow ecosystem itself can adapt to climate change. At Bunkeflo salt meadows, the vegetation will need to adapt to higher water levels and possibly also withstand higher energy waves. In principle, for the salt meadow to remain in place the elevation gain rate by soil building must be greater than the rate of sea level rise (Kirwan & Megonigal, 2013). Elevation gain is a result of biological and physical feedback-loops that determine the so-called accretion rate (the rate at which the soil surface increases). Plants play an important role in these feedback-loops since they can increase mineral sedimentation by lowering water velocities (Kirwan & Megonigal, 2013). Importantly, they also add organic matter both above and below the soil surface (Kirwan & Megonigal, 2013). The root systems of plants also stabilize the soil, hence reducing erosion (Willemsen, 2020).

A meta-analysis by Kirwan et al. (2016) concluded that historically, coastal marshes have often been building soil at rates similar to or exceeding sea level rise.

Furthermore, using process-based models they predict that marshes generally will survive under a wide range of future sea level rise scenarios (Kirwan et al., 2016). Other research related specifically to the habitat of Atlantic salt meadows has found that the vertical accretion rate of salt meadows theoretically may be high enough to cope with relative sea level rise of up to 6 mm per year (Doody et al., 2008). However, it is also emphasised that in some areas, accretion rates of salt meadows are already too low relative to sea level rise and consequently the vegetation becomes permanently inundated and may disappear (Doody et al., 2008). These conclusions make it difficult to predict the fate of the salt meadows at Bunkeflo, but they are an important reminder that natural ecosystems can and have adapted successfully to changing environmental conditions. To increase the chances that Bunkeflo salt meadows adapt to climate change, measures can be taken to increase accretion rates of soil or reduce erosion. Such strategies could include beach nourishment, planting of salt marsh grasses or constructing wave breakers or groynes.

If the habitat cannot retain its current location seaward, the plant communities may migrate to higher elevation. It has been suggested that wetland migration could largely offset the loss of these ecosystems if there are no anthropogenic barriers (e.g. dikes) (Kirwan & Megonigal, 2013). When the retreat is blocked by anthropogenic structures or actions, there may be no space for the ecosystems to retreat. This is known as "coastal squeeze". Therefore, Kirwan & Megonigal (2013) emphasise that the fate of coastal wetlands may be more dependent on the adaptation strategies used to protect coastal infrastructure and communities from climate change, rather than the direct consequences of climate change itself.

In the case of Bunkeflostrand, the human settlements already prevent any significant landward migration, but a sea dike would most likely seal off the salt meadows and marshes even more. Because of sea level rise, a dike will likely be needed, and through the damping effect of the salt meadows an added safety dimension to the dike is in place. However, due to the uncertain future of the marshes, and the difficulties involved in calculating wave damping by vegetation, one could question whether this effect should be considered at all when designing a dike. As has been argued by van Loon-Steensma and Kok (2016), taking the damping effect into account may actually increase flooding risk. They argue that since vegetation does dampen waves, not taking it into account will lead to over-dimensioned dikes, which reduces risk. However, if the damping effect is considered, the variable nature of the damping effect over time could lead to an under-dimensioned dike, which increases risk. However, it should be emphasized once more that, as long as they are intact, salt meadows and salt marshes do reduce

wave heights and thus contribute to coastal protection. It is therefore important to protect such ecosystems. Where vegetation is not already present, it could be an option to establish plant communities to gain the protective effects mentioned. However, this may require a lot of space, and if vegetation is not present naturally it is important to ask why this is the case and whether planted vegetation will be able to successfully establish.

In the case of Bunkeflostrand, several areas are already covered by dense and tall reeds, and since reed has the highest damping, at least under high water levels, it seems appropriate to maintain reed beds in areas that are very exposed to wave action. Strandhem is such an area that is topographically low and very close to the coast. At present, there is a 70 – 80 m wide reed bed separating Strandhem from the ocean. It is the opinion of the authors that these reed beds should be maintained, and that grazing should not be allowed there to ensure the protection of the dike at Strandhem. Since damping is nonlinear, with most damping occurring in the beginning of transects, a relatively thin strip of reed could be established along the shoreline of the grazed meadows to relieve part of the wave damping. However, this could interfere with accretion processes by blocking the deposition of seaweed, discussed later in this section.

In this thesis, only the wave damping effect of vegetated foreshores has been studied. It is important to emphasise that the vegetation also provides other important coastal protection services. A meta-analysis by Shepard et al. (2011) concluded that salt marsh vegetation has a significantly positive effect on shoreline stabilization by reducing erosion and increasing accretion. They also note that these ecosystems can be important for floodwater attenuation, but these effects are more challenging to quantify. Wave-vegetation interactions also affect infragravity-band waves and wave setup, which can be important parameters to consider for coastal risk assessment (Rooijen et al., 2016).

Beyond coastal protection services, salt meadows provide many other important ecosystem services. In some cases, the optimisation of one service may compromise another. At Bunkeflo salt meadows, biodiversity is high and therefore is identified as an important value to protect. The grazed meadows are especially diverse and provide unique conditions for rare flora and fauna. On the other hand, in this thesis, less diverse plant communities (i.e., reed and high grass) are identified as the most valuable habitats for wave damping. Therefore, it seems that there may be a trade-off between coastal protection and biodiversity. However, these values may be more intrinsically related and complex than it seems. As mentioned previously, spatial variability of the terrain may be an important factor to increase wave damping. In many areas of the grazed meadows, tussock or bunched grasses can

be found, creating stable tufts (Figure 16). Furthermore, when cattle graze the meadows they step in between the mounds, presumably creating even deeper suppressions between the tufts. Geese also graze the open meadows. As they do so, they deposit organic matter and plant nutrients on the soil through excretion. Possibly, this may further increase the growth rate of plants and influence the long-term soil building rate of the meadows. During site visits, it has also been observed that seaweed and eel grass is deposited on the meadows. Since dense vegetation such as reed and high grass may trap the seaweed at the shoreline, the grazed salt meadows may allow for the deposition of this debris further onshore, possibly also increasing soil building rates. Consequently, it is possible that the grazed meadows are more resilient to sea level rise than the other habitats and may also contribute to wave damping when tufts of grass create an uneven topography. Even though these feed-back loops are speculative, they are important examples to highlight the complexity of determining which habitats provide the most long-term coastal protection.

7 Conclusions

This thesis has attempted to quantify wave damping from vegetation at Bunkeflostrand by using a biomass-based method developed by Maza et al. (2020). The study was divided into hypothetical cases and a case study. The former studied different parameters in isolation in short transects while the latter applied the biomass method to four different transects at Bunkeflostrand under different scenarios of sea level rise and extreme wave heights.

A wave damping computation framework was developed by following the steps presented in Figure 17. The computation process is suitable for areas with varied vegetation but may require additional validation and calibration. All required software is free, and the field methods are simple. First, the area should be classified into general vegetation types and the height and dry weight biomass of each vegetation type measured. Using the mobile app QField on-site is recommended as an effective way to classify the area and facilitate the GIS-processing step. Then hydrodynamic scenarios must be defined, and geographical data of topography and bathymetry obtained. Thereafter, transects are drawn in GIS software over the data layers containing the vegetation classification, topography and bathymetry. After this, data can be extracted from these layers by generating data points along the transects. The information from these data points is then saved in a CSV-file. Finally, the CSV-file is imported to a script written in Python and the wave heights along the transects are calculated.

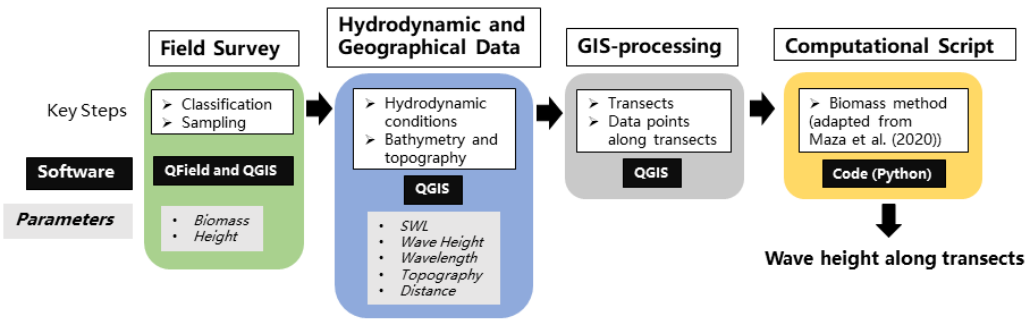

Figure 17. Steps of the developed computational process to calculate wave damping for field conditions based on the biomass method by Maza et al. (2020).

The research questions presented in section 1.1 are answered as follows:

How much wave damping can be expected from the salt meadows at Bunkeflostrand?

The results in this thesis indicate that the wave damping capacity of the studied vegetation types at Bunkeflostrand is high, especially where cross shore distances are great or where a lot of reed is present. The reduction in wave heights at the end of transects ranged from 65.6 % to 94.6 %, where the greatest value was attained at the end of the longest transect for the lowest water level. However, it is difficult to determine whether the results are reasonable. Literature values vary greatly depending mainly on hydrodynamic conditions and type of vegetation, meaning it is difficult to compare directly, but applying the biomass method to data from other studies suggests that it overestimates the wave damping by 27.5 % - 39.2 %.

It is important to mention that large areas of the salt meadows have been omitted from the study since they were deemed unsuitable for the biomass method. This includes mudflats, the meadows that have lowest vegetation due to grazing, as well as areas with trees, shrubs and bushes. Assuming that the same parameters govern these types of vegetation as the ones that were studied, it is likely that the mudflats and low meadows have lower damping capacity compared to the other vegetation types. This is because they have low vegetation heights and low biomass, with the mudflats probably having the lowest damping compared to the grazed meadows. Similarly, it can be assumed that the forested areas have a high damping capacity since the vegetation is high, biomass is high, and the vegetation is very rigid.

The biomass method used in this thesis has only been validated for low wave heights and water depths, whereas the scenarios in the case study have much greater depths and wave heights. Large waves could cause plant stems to fold over or break which would limit the wave damping capacity. Hence, the wave height reductions mentioned above should be used with caution. Additionally, it is not clear to what extent the salt meadows will be able to adapt to sea level rise, which means that the location of the shoreline, as well as the distribution of the different vegetation types, will change over time. A landward migrating shoreline implies a decreasing cross-shore extent of the salt meadows and hence a lower wave damping capacity.

What are the most important parameters influencing wave damping, related to hydrodynamic conditions and vegetation characteristics at Bunkeflo salt meadows?

It was found that longer transects and lower water levels lead to greater wave height reductions in the case study. The hypothetical cases showed that the ratio of vegetation height to water depth was especially important, and that emergent vegetation dampens waves more effectively than submerged vegetation. The biomass density of the vegetation is also important, but if the vegetation is very low the wave damping is mainly determined by the water depth. Hence high grass showed damping on a par with reed when the water depth was 0.5 m, but at greater water depths the reed was significantly more effective due to its taller canopy. Hence an effective salt meadow from a wave damping perspective would have reed beds in low-lying areas and dense grasses in higher terrain. Assuming a constant foreshore slope this means establishing reed close to the shore and high grass in more landward areas. An important consideration is that the results in this thesis do not necessarily reflect how real vegetation responds to certain waves and water depths, but rather show how the equations respond to changing parameters. Similarly, using biomass as a proxy means that some characteristics that are important for wave damping, such as stem flexibility, are not accurately taken into account. This is an inherent weakness in empirical relationships that do not reflect the actual physical processes involved.

7.1 Recommendations

With the current knowledge, it is difficult to precisely quantify wave damping by vegetation without validation from field measurements. Consequently, it is not recommended to design coastal protection infrastructure based on the results presented in this report. The biomass method needs to be further developed and validated to include shoaling and higher wave energies before being used for design purposes. Despite the uncertainties, the results do support that wave damping from vegetation is likely to be high. Hence, it is important to acknowledge coastal vegetation as an important nature-based engineering solution.

In order to maximize wave damping from vegetation, it is recommended that engineers and decision makers managing coastal wetlands consider the following:

- Reserve vegetated buffer zones in front of dikes. Wider buffer zones dampen waves more, but since most damping happens at the beginning of transects even short buffer zones are important for coastal protection.
- Allow the establishment of tall and dense vegetation, such as *Phragmites* reeds, at exposed areas, especially when wide buffer zones are not possible.
- Refrain from allowing grazing at Strandhem for the reason mentioned above.

Finally, it is important to remember that salt meadows and salt marshes provide many other ecosystem services besides wave damping. Their ability to adapt to rising sea levels, treat water and provide habitat for a multitude of plants and animals should not be overlooked. By knowing what the salt meadows can do for us, we can take steps to understand how we can manage and protect them.

8 References

Adell, A., Nunes de Brito Junior, A., Almström, B., Goodfellow, B., Bokhari Irminger, S., Hallin, C., & Nyberg, J. (2021). Open-access Portal with Hindcast Wave Data for Skåne and Halland. *Vatten: Tidskrift För Vattenvård /Journal of Water Management and Research*, *77*(2).

Almström, B., Street, S. I., Schmidt, E., & Boonzaaier, B. (2017). *Strategi mot extrema högvatten i Malmö: Delområde 4—Söder om Öresundsbron*. Sweco.

Anderson, M. E., Smith, J. M., & McKay, S. K. (2011). *Wave Dissipation by Vegetation*. Defense Technical Information Center. https://doi.org/10.21236/AD1003881

Augustin, L. N., Irish, J. L., & Lynett, P. (2009). Laboratory and numerical studies of wave damping by emergent and near-emergent wetland vegetation. *Coastal Engineering*, *56*(3), 332–340. https://doi.org/10.1016/j.coastaleng.2008.09.004

Balke, T., Klaassen, P. C., Garbutt, A., van der Wal, D., Herman, P. M. J., & Bouma, T. J. (2012). Conditional outcome of ecosystem engineering: A case study on tussocks of the salt marsh pioneer Spartina anglica. *Geomorphology*, *153–154*, 232–238. https://doi.org/10.1016/j.geomorph.2012.03.002

Blackburn, S., Pelling, M., & Marques, C. (2019). Chapter 38 - Megacities and the Coast: Global Context and Scope for Transformation. In E. Wolanski, J. W. Day, M. Elliott, & R. Ramachandran (Eds.), *Coasts and Estuaries* (pp. 661–669). Elsevier. https://doi.org/10.1016/B978-0-12-814003-1.00038-1

Blackmar, P. J., Cox, D. T., & Wu, W.-C. (2014). Laboratory Observations and Numerical Simulations of Wave Height Attenuation in Heterogeneous Vegetation. *Journal of Waterway, Port, Coastal, and Ocean Engineering*, *140*(1), 56–65. https://doi.org/10.1061/(ASCE)WW.1943-5460.0000215

Bouma, T. J., Friedrichs, M., Wesenbeeck, B. K. V., Temmerman, S., Graf, G., & Herman, P. M. J. (2009). Density-dependent linkage of scale-dependent feedbacks: A flume study on the intertidal macrophyte Spartina anglica. *Oikos*, *118*(2), 260–268. https://doi.org/10.1111/j.1600-0706.2008.16892.x

Bouma, T. J., Vries, M. B. D., & Herman, P. M. J. (2010). Comparing ecosystem engineering efficiency of two plant species with contrasting growth strategies. *Ecology*, *91*(9), 2696–2704. https://doi.org/10.1890/09-0690.1

Cohen-Shacham, E., Walters, G., Janzen, C., & Maginnis, S. (2016). *Nature-based Solutions to address global societal challenges*. IUCN. https://portals.iucn.org/library/sites/library/files/documents/2016-036.pdf

Dalrymple, R. A., Kirby, J. T., & Hwang, P. A. (1984). Wave Diffraction Due to Areas of Energy Dissipation. *Journal of Waterway, Port, Coastal, and Ocean Engineering*, *110*(1), 67–79. https://doi.org/10.1061/(ASCE)0733-950X(1984)110:1(67)

Doody, J. P., European Commission, & Directorate-General for the Environment. (2008). *Management of Natura 2000 habitats: Atlantic salt meadows (Glauco-Puccinellietalia maritimae) 1330 : Directive 92/43/EEC on the conservation of natural habitats and of wild fauna and flora.* European Commission. http://ec.europa.eu/environment/nature/natura2000/management/habitats/pdf/1330_Atlantic_salt_meadows.pdf

Doughty, C. L., & Cavanaugh, K. C. (2019). Mapping Coastal Wetland Biomass from High Resolution Unmanned Aerial Vehicle (UAV) Imagery. *Remote Sensing*, *11*(5), 540. https://doi.org/10.3390/rs11050540

Emanuelson, J., & Holmquist, A. (2019). *Strukturplan Bunkeflostrand—Slutsatser av medborgardialog. Underlag för aktualisering av översiktsplan och fortsatt planering.* 20.

EurOtop. (2018). *EurOtop—Manual on wave overtopping of sea defences and related structures. An overtopping manual largely based on European research, but for worldwide application. Second edition 2018*. http://www.overtopping-manual.com/assets/downloads/EurOtop_II_2018_Final_version.pdf

Feagin, R. A., Irish, J. L., Möller, I., Williams, A. M., Colón-Rivera, R. J., & Mousavi, M. E. (2011). Short communication: Engineering properties of wetland plants with application to wave attenuation. *Coastal Engineering*, *58*(3), 251–255. https://doi.org/10.1016/j.coastaleng.2010.10.003

Foster-Martinez, M. R., Alizad, K., & Hagen, S. C. (2020). Estimating wave attenuation at the coastal land margin with a GIS toolbox. *Environmental Modelling & Software*, *132*, 104788. https://doi.org/10.1016/j.envsoft.2020.104788

Garzon, J. L., Maza, M., Ferreira, C. M., Lara, J. L., & Losada, I. J. (2019). Wave Attenuation by Spartina Saltmarshes in the Chesapeake Bay Under Storm Surge Conditions. *Journal of Geophysical Research: Oceans*, *124*(7), 5220–5243. https://doi.org/10.1029/2018JC014865

Gedan, K. B., Kirwan, M. L., Wolanski, E., Barbier, E. B., & Silliman, B. R. (2011). The present and future role of coastal wetland vegetation in protecting shorelines: Answering recent challenges to the paradigm. *Climatic Change*, *106*(1), 7–29. https://doi.org/10.1007/s10584-010-0003-7

Jönsson, A., & Jönsson, S. (2015). Strandhemliv: Del 5: Sonja och Alwe Jönssons Strandhem. *Strandhemliv*. http://strandhemliv.blogspot.com/2015/01/del-5-sonja-och-alwe-jonssons-strandhem.html

Kirwan, M. L., & Megonigal, J. P. (2013). Tidal wetland stability in the face of human impacts and sea-level rise. *Nature*, *504*(7478), 53–60. https://doi.org/10.1038/nature12856

Kirwan, M. L., Temmerman, S., Skeehan, E. E., Guntenspergen, G. R., & Fagherazzi, S. (2016). Overestimation of marsh vulnerability to sea level rise. *Nature Climate Change*, *6*(3), 253–260. https://doi.org/10.1038/nclimate2909

Länsstyrelsen Skåne. (n.d.). *Bunkeflo strandängar* [Text]. Retrieved May 21, 2021, from https://www.lansstyrelsen.se/skane/besoksmal/naturreservat/malmo/bunkeflo-strandangar.html

Länsstyrelsen Västra Götaland. (2020). Strategi för skydd och förvaltning av marina miljöer och arter i Västerhavet. *2020:14*, 254.

Losada, I. J., Maza, M., & Lara, J. L. (2016). A new formulation for vegetation-induced damping under combined waves and currents. *Coastal Engineering*, *107*, 1–13. https://doi.org/10.1016/j.coastaleng.2015.09.011

Malmö stad. (n.d.). *Skötselplan för naturreservatet Bunkeflo strandängar*. https://malmo.se/download/18.45c7aab61662eba4dac4c52/1538987026135/3.pdf

Malmö stad. (2020). *Såhär arbetar Malmö Stad med kustskydd* [Text]. https://malmo.se/Aktuellt/Artiklar-Malmo-stad/2020-02-07-Sa-har-arbetar-Malmo-stad-med-kustskydd.html

Malmö Stadsbyggnadskontor. (2008). *Klimatet, havsnivån och planeringen—Dialog PM Malmö stad*. yumpu.com. https://www.yumpu.com/sv/document/view/9679572/klimatet-havsnivan-och-planeringen-dialog-pm-malmo-stad

Maza, M. (2020, November 25). *Session #113 - Maria Maza: Ecosystem Biomass as a Key Parameter Determining its Coastal Protection*. https://www.youtube.com/watch?v=-qaKkBWZApk&feature=youtu.be

Maza, M. (2021, April 9). *Adapting biomass equation to field conditions (Master Thesis)* [Personal communication].

Maza, M., Lara, J. L., & Losada, I. J. (2015). Tsunami wave interaction with mangrove forests: A 3-D numerical approach. *Coastal Engineering*, *98*, 33–54. https://doi.org/10.1016/j.coastaleng.2015.01.002

Maza, M., Lara, J. L., Losada, I. J., Ondiviela, B., Trinogga, J., & Bouma, T. J. (2015). Large-scale 3-D experiments of wave and current interaction with real vegetation. Part 2: Experimental analysis. *Coastal Engineering*, *106*, 73–86. https://doi.org/10.1016/j.coastaleng.2015.09.010

Maza, M., Lopez-Arias, F., Lara, J. L., & Losada, I. J. (2020). Ecosystem Biomass as a Key Parameter Determining its Coastal Protection Service. *Coastal Engineering Proceedings*, *36v*, 29–29. https://doi.org/10.9753/icce.v36v.management.29

Mendez, F. J., & Losada, I. J. (2004). An empirical model to estimate the propagation of random breaking and nonbreaking waves over vegetation fields. *Coastal Engineering*, *51*(2), 103–118. https://doi.org/10.1016/j.coastaleng.2003.11.003

Millennium Ecosystem Assessment (Ed.). (2005). *Ecosystems and human well-being: Wetlands and water synthesis: a report of the Millennium Ecosystem Assessment*. World Resources Institute.

Möller, I. (2006). Quantifying saltmarsh vegetation and its effect on wave height dissipation: Results from a UK East coast saltmarsh. *Estuarine, Coastal and Shelf Science*, *69*(3), 337–351. https://doi.org/10.1016/j.ecss.2006.05.003

Möller, I., Kudella, M., Rupprecht, F., Spencer, T., Paul, M., van Wesenbeeck, B. K., Wolters, G., Jensen, K., Bouma, T. J., Miranda-Lange, M., & Schimmels, S. (2014). Wave attenuation over coastal salt marshes under storm surge conditions. *Nature Geoscience*, *7*(10), 727–731. https://doi.org/10.1038/ngeo2251

Möller, I., Mantilla-Contreras, J., Spencer, T., & Hayes, A. (2011). Micro-tidal coastal reed beds: Hydro-morphological insights and observations on wave transformation from the southern Baltic Sea. *Estuarine, Coastal and Shelf Science*, *92*(3), 424–436. https://doi.org/10.1016/j.ecss.2011.01.016

Möller, I., & Spencer, T. (2002). Wave dissipation over macro-tidal saltmarshes: Effects of marsh edge typology and vegetation change. *Journal of Coastal Research*, *36 (10036)*, 506–521. https://doi.org/10.2112/1551-5036-36.sp1.506

Möller, I., Spencer, T., French, J. R., Leggett, D. J., & Dixon, M. (1999). Wave Transformation Over Salt Marshes: A Field and Numerical Modelling Study from North Norfolk, England. *Estuarine, Coastal and Shelf Science*, *49*(3), 411–426. https://doi.org/10.1006/ecss.1999.0509

Naturvårdsverket. (2011). *Salta strandängar*. Naturvårdsverket; NV-04493-11. https://www.naturvardsverket.se/upload/stod-i-miljoarbetet/vagledning/natura-2000/naturtyper/kust-och-hav/vl-1330-saltstrandang.pdf

Nielsen, P. (2009). *Coastal and Estuarine Processes* (Vol. 29). World Scientific Publishing Co Pte Ltd.

OPENGIS.ch. (2021). *QField* (1.9.5) [Android]. OPENGIS.ch. https://play.google.com/store/apps/details?id=ch.opengis.qfield&hl=en&gl=US

Paquier, A.-E., Haddad, J., Lawler, S., & Ferreira, C. M. (2017). Quantification of the Attenuation of Storm Surge Components by a Coastal Wetland of the US Mid Atlantic. *Estuaries and Coasts*, *40*(4), 930–946. https://doi.org/10.1007/s12237-016-0190-1

Paul, M., & Amos, C. L. (2011). Spatial and seasonal variation in wave attenuation over Zostera noltii. *Journal of Geophysical Research: Oceans*, *116*(C8). https://doi.org/10.1029/2010JC006797

Paul, M., Bouma, T., & Amos, C. (2012). Wave attenuation by submerged vegetation: Combining the effect of organism traits and tidal current. *Marine Ecology Progress Series*, *444*, 31–41. https://doi.org/10.3354/meps09489

Reinsch et al. (n.d.). *2.1.1 Aboveground plant biomass – ClimEx Handbook*. Retrieved April 8, 2021, from https://climexhandbook.w.uib.no/2019/11/06/aboveground-plant-biomass/

Rooijen, A. A. V., Van, J. S. M., Vries, T. D., Mccall, R. T., Dongeren, A. R. V., Roelvink, J. A., & Reniers, A. J. H. M. (2015). *1 Modeling of Wave Attenuation by Vegetation with Xbeach*.

Rooijen, A. A. V., McCall, R. T., Vries, J. S. M. van T. de, Dongeren, A. R. van, Reniers, A. J. H. M., & Roelvink, J. A. (2016). Modeling the effect of wave-vegetation interaction on wave setup. *Journal of Geophysical Research: Oceans*, *121*(6), 4341–4359. https://doi.org/10.1002/2015JC011392

Rupprecht, F., Möller, I., Paul, M., Kudella, M., Spencer, T., van Wesenbeeck, B. K., Wolters, G., Jensen, K., Bouma, T. J., Miranda-Lange, M., & Schimmels, S. (2017). Vegetation-wave interactions in salt marshes under storm surge conditions.

Ecological Engineering, *100*, 301–315. https://doi.org/10.1016/j.ecoleng.2016.12.030

SCB. (2021). *Folkmängd och landareal i tätorter, per tätort. Vart femte år 1960—2020*. Statistikdatabasen. http://www.statistikdatabasen.scb.se/pxweb/sv/ssd/START__MI__MI0810__MI0810A/LandarealTatortN/

Shepard, C. C., Crain, C. M., & Beck, M. W. (2011). The Protective Role of Coastal Marshes: A Systematic Review and Meta-analysis. *PLOS ONE*, *6*(11), e27374. https://doi.org/10.1371/journal.pone.0027374

Simonsson, L., & Liljedahl, B. (2017). *Höga havsnivåer och översvämningar*. 105.

SMHI. (2018). *Extremvattenstånd i Malmö* (2018/955/9.5).

SMHI. (2020). *Framtida medelvattenstånd*. https://www.smhi.se/klimat/stigande-havsnivaer/framtida-medelvattenstand-1.165493

Spalding, M., Ruffo, S., Lacambra, C., Meliane, I., Hale, L., Shepard, C., & Beck, M. (2014). The role of ecosystems in coastal protection: Adapting to climate change and coastal hazards. *Ocean & Coastal Management*, *90*, 50–57. https://doi.org/10.1016/j.ocecoaman.2013.09.007

Sutton-Grier, A. E., Wowk, K., & Bamford, H. (2015). Future of our coasts: The potential for natural and hybrid infrastructure to enhance the resilience of our coastal communities, economies and ecosystems. *Environmental Science & Policy*, *51*, 137–148. https://doi.org/10.1016/j.envsci.2015.04.006

Suzuki, T., Zijlema, M., Burger, B., Meijer, M. C., & Narayan, S. (2012). Wave dissipation by vegetation with layer schematization in SWAN. *Coastal Engineering*, *59*(1), 64–71. https://doi.org/10.1016/j.coastaleng.2011.07.006

USACE. (1984). *Shore Protection Manual Volume I* (4th Edition, Vol. 1–Volume I). Department of the Army. http://ft-sipil.unila.ac.id/dbooks/S%20P%20M%201984%20volume%201-1.pdf

Van Loon-Steensma, J. M., & Kok, M. (2016). Risk reduction by combining nature values with flood protection? *E3S Web of Conferences*, *7*, 13003. https://doi.org/10.1051/e3sconf/20160713003

van Veelen, T. (2020, November 26). *Session #113 - Thomas van Veelen: Nature based coastal protection wave damping by salt marsh*. https://www.youtube.com/watch?v=AjnFx3aFSzs&feature=youtu.be

van Veelen, T. J., Fairchild, T. P., Reeve, D. E., & Karunarathna, H. (2020). Experimental study on vegetation flexibility as control parameter for wave damping and velocity structure. *Coastal Engineering*, *157*, 103648. https://doi.org/10.1016/j.coastaleng.2020.103648

Wamsley, T. V., Cialone, M. A., Smith, J. M., Ebersole, B. A., & Grzegorzewski, A. S. (2009). Influence of landscape restoration and degradation on storm surge and waves in southern Louisiana. *Natural Hazards*, *51*(1), 207–224. https://doi.org/10.1007/s11069-009-9378-z

Willemsen, P. W. J. M. (2020). *Biogeomorphology of salt marshes: Understanding the decadal salt marsh dynamics for flood defense*. https://doi.org/10.3990/1.9789036551120

Wu, W.-C., & Cox, D. T. (2015). Effects of wave steepness and relative water depth on wave attenuation by emergent vegetation. *Estuarine, Coastal and Shelf Science*, *164*, 443–450. https://doi.org/10.1016/j.ecss.2015.08.009

Yang, S. L., Li, H., Ysebaert, T., Bouma, T. J., Zhang, W. X., Wang, Y. Y., Li, P., Li, M., & Ding, P. X. (2008). Spatial and temporal variations in sediment grain size in tidal wetlands, Yangtze Delta: On the role of physical and biotic controls. *Estuarine, Coastal and Shelf Science*, *77*(4), 657–671. https://doi.org/10.1016/j.ecss.2007.10.024

Yang, Y., & Irish, J. L. (2018). Evolution of wave spectra in mound-channel wetland systems. *Estuarine, Coastal and Shelf Science*, *207*, 444–456. https://doi.org/10.1016/j.ecss.2017.06.012

Ysebaert, T., Yang, S.-L., Zhang, L., He, Q., Bouma, T. J., & Herman, P. M. J. (2011). Wave Attenuation by Two Contrasting Ecosystem Engineering Salt Marsh Macrophytes in the Intertidal Pioneer Zone. *Wetlands*, *31*(6), 1043–1054. https://doi.org/10.1007/s13157-011-0240-1

A Appendix

A1 Calculation Method Development

With regards to the empirical equation developed by Maza et al. (2020) there are a number of calculation issues that needed resolving in order to apply the equations to field conditions.

Firstly, the equations presented assume that the depth is constant, i.e. no slope. Even though most salt meadows may have rather gentle foreshore slopes, it is evident that even a gentle slope will result in a reduced water depth, since the cross-shore distances typically are long. The change in depth consequently effects the wave damping by: i) shoaling and breaking and ii) changing the submergence of the vegetation and the wave height-depth ratio in Eq. (3).

i) In relation to shoaling and breaking, Mendez and Losada (2004) developed Eq. (1) (as mentioned in section 3.1). However, since the derived equations are expressed in relation to the drag coefficient, they do not offer a direct solution in relation to method presented by Maza et al. (2020). Therefore, shoaling and breaking have not been included in the calculation method used in this thesis.

ii) A solution to take the depth change into consideration in Eq. (1) and (3) is to perform the calculation "step-wise" by dividing the total cross-shore distance into segments. Thereby, the depth will be better approximated for each segment, solving issue (ii) if the segments are short (but not solving (i)). The method is illustrated in Figure 7.

Secondly, vegetation in the field is often heterogeneous and the vegetation type may change moving cross-shore. Therefore, the damping coefficient will change and the vegetation height and biomass parameters must be updated accordingly (Eq. (3)).

Thirdly, to increase the accuracy of the damping coefficient along the transect it seems necessary to update H_i and L in Eq. (3), since these parameters decrease as the wave is dampened. This is especially relevant for long transects, where H_i and L may have changed significantly moving cross-shore.

Considering the three issues above, the damping coefficient will change moving cross-shore and therefore the calculation of the damping coefficient must be iterated for each segment of the total cross-shore distance. However, inserting β-values stepwise in Eq. (1) results in discontinuities if x is continuous (red graph in

Figure 18). Furthermore, the calculation also becomes sensitive to the number of iterations, i.e., length of the segments. This problem is not unique to the method developed by Maza et al. (2020) but is shared by all vegetation damping models seeking an analytical solution based on the equations by either Kobayashi et al. (1993) (Eq. (2)) or Dalrymple et al. (1984) (Eq. (1)). This is because the derivation of these wave decay equations is based on the premises that β can be assumed constant over the entire transect.

A solution to the discontinuities could be to set $x = 0$ at the start of each segment along the transect and change H_0 in Eq. (1) to H_{n-1} as presented below.

$$H(x) = \frac{H(x_{n-1})}{1 + \beta x_n} \tag{12}$$

where H_{n-1} indicates the wave height at segment number $\mathrm{n} - 1$.

This is similar to the solution presented by Foster-Martinez et al. (2020, p. 4). However, since Eq. (1) is not linear, subdividing it into smaller segments for iteration will increase the wave damping (green versus black graph Figure 18). This is because the damping is greatest when x is smallest in Eq. (1). This method is therefore also dependent on the number of segments. We therefore question this approach and seek other solutions based on the constraint that x must be continuous.

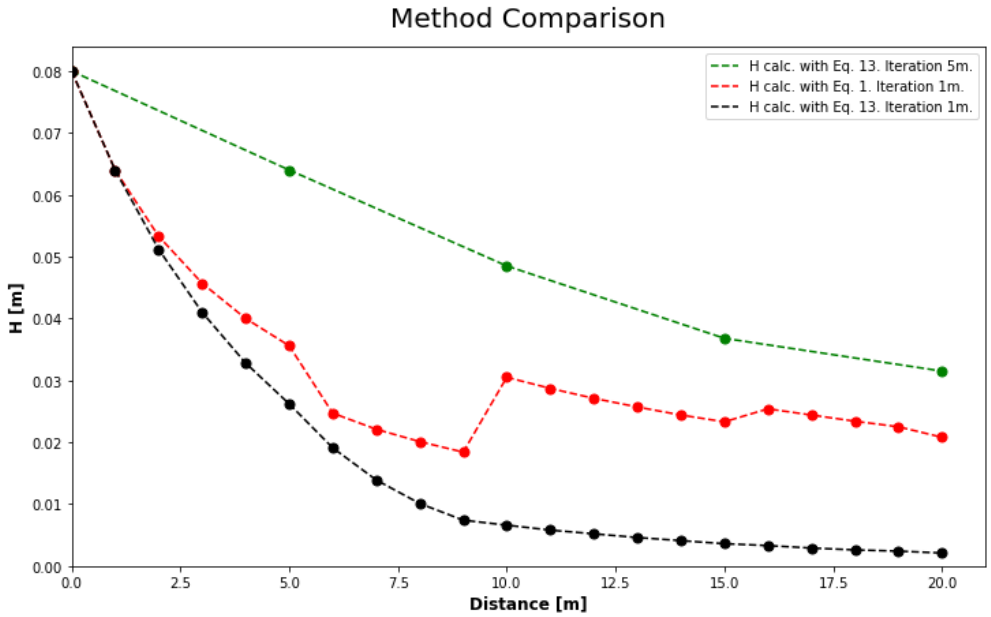

Figure 18. The calculation method based on Eq. (1) (red) and Eq. (12) (green and black) are compared. The hypothetical scenario is: first 5m low reed, then 10m high grass and finally another 5m low reed. Depth is constant (=20 cm) and incident wave height H_0=8 cm. β is updated each iteration according to the linear relation presented by Maza (2020) (Eq. (3)). Note that the dashed line between the points is only used to illustrate that the direction of change between the points. It is not a representation of the actual wave heights in between the points.

The following two equation modifications were developed and compared (Figure 19):

Alt. 1: Replace H_0 with $H_{0,n}$

Eq. (1) is modified by changing the incoming wave height (H_0) to a re-calculated incoming wave height ($H_{0,n}$) depending on β at the current segment (as presented in section 4.4.3):

$$H(x_n) = \frac{H_{0,n}}{1 + \beta_n x_n} \tag{7}$$

$$H_{0,n} = H(x_{n-1}) * (1 + \beta_n x_{n-1}) \tag{8}$$

Alt. 2: Add m-value

Eq. (1) is modified by the addition of an m-value compensating for the differences between the current and previous segment if β changes.

$$H(x_n) = \frac{H_0}{1 + \beta_n x_n} + m \tag{13}$$

$$m = H(x_{n-1}) - \frac{H_0}{1 + \beta_n x_{n-1}} \tag{14}$$

Both solutions above resolve both the discontinuities and the dependence of segment lengths. However, neither of these methods have been validated or derived from physical laws and therefore it is not possible to determine which one is more valid. Yet another alternative beyond, to the two above, is to calculate a representative weighted value of β for the entire transect. However, this method was considered inaccurate and was therefore not explored further. As a conservative measure, the authors of this thesis have opted for using the method of re-calculating H_0 (Alt. 1) since this method generally resulted in less damping. However, even with the suggested methods, some issues remain as will be explained below.

As mentioned in section 6.2, not all areas of the salt meadows have vegetation characteristics that match the requirements of Eq. (3). Therefore, to create a computational framework applicable to more vegetation types it may be necessary to use multiple calculation methods, even along the same individual transects. However, this raises other issues. Since Eq. (1) is a rational function of the distance x into the vegetation field (i.e. non-linear), it is important to define when the vegetation field "starts" and when it is "discontinued". For example, considering an area with little or no vegetation (e.g. low meadow) in front of the area with vegetation (e.g. high grass), it becomes difficult to determine when to define the start of x into the vegetation field. This is an inherent problem of the Eq. (1) and no solution is suggested. As mentioned previously, in this thesis we avoided the problem by simply excluding the areas of the salt marshes where these uncertainties arise.

Finally, as discussed in section 6.1.5, the last modification of the calculation method was to replace Eq. (3) with Eq. (9). In Figure 19 below, the four different plausible calculation method combinations are compared along transect number 2 from the case study.

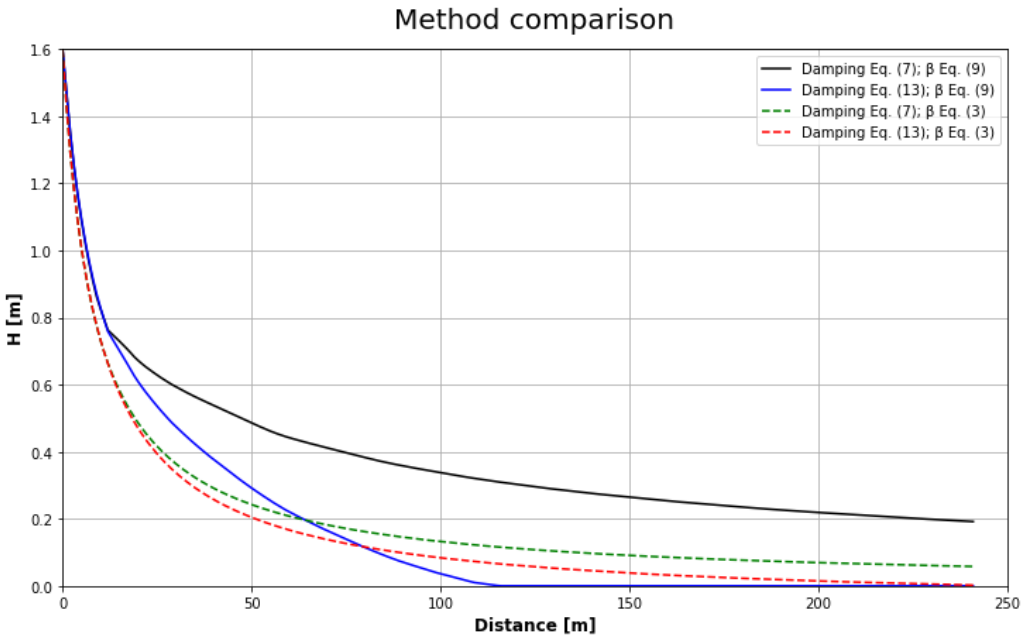

Figure 19. The results from the four possible combinations of the new equation methods are plotted for transect 2. Incident wave height is 1.6 and SWL is 2.17 m (RH2000). Iteration interval every meter.

As can be seen in Figure 19, the two curves (dashed green and red) using Maza et al. (2020) linear fit (Eq. (3)) are quite similar. This is a consequence of the dominating 0.1 term in Eq. (3). However, when applying our fit (Eq. (9)), the two calculation methods differ significantly. This highlights the importance of further understanding how, or even if, the damping equation by Dalrymple et al. (1984) (Eq. (1)) can be segmentized to account for varied damping along a cross-shore transect.

A2 Inundation Levels for 2050

The future extreme water levels assume that the water level with a 100-year return period has the same elevation above mean sea level in all scenarios, which according to SMHI (2020) is 141 cm in Klagshamn. Hence, any increase in water level is due to sea level rise. Additionally, land rise due postglacial isostatic rebound has also been included.

The water level with a 100-year return period for the years 2021 and 2100 has been obtained from SMHI (2018). The water level for the year 2050 has been calculated according to

Level 2050 = 141 cm + sea level rise until 2050 – land rise until 2050 + 12 cm

= 141 cm + 34 cm

= 175 cm in RH 2000

The value of 34 cm comes from SMHI (2020) and includes regional sea level rise until 2050, local land rise due to isostatic rebound, as well as 12 cm to get a value in RH 2000. RH 2000 is the national height system in Sweden. At Klagshamn, the mean sea water level is 12 cm in RH 2000, which is the reason for adding 12 cm to the calculation above.

A3 Vegetation Sampling

Figure 20 shows the locations of the vegetation sampling points. Locations for sampling were chosen in order to make samples representative of the vegetation type in general, and of the polygon where the sample was taken in particular.

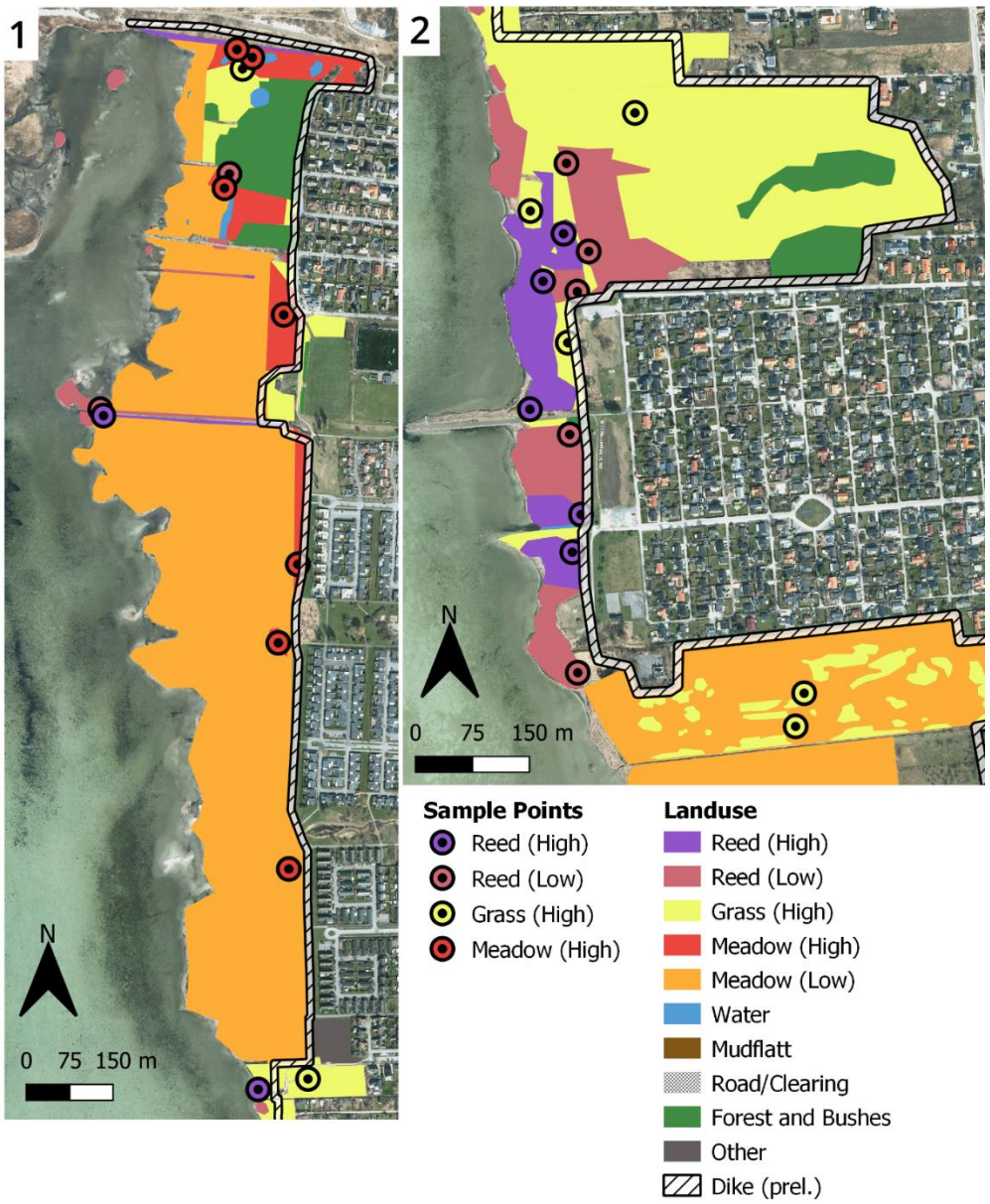

Figure 20. Sample points of biomass and hight. Seven points within each of the four selected vegetation types.

Table 12 shows the raw data from the vegetation sampling, as well as mean value, standard deviation and 95 % confidence interval (CI) devation from the mean for biomass and vegetation height for each vegetation type.

The 95 % CI were calculated according to

$$\mathrm{CI} = \mathrm{mean} \pm t_{95} \frac{standard\ deviation}{\sqrt{n}}$$

Where n is the sample size, which equals 7 for all vegetation types. The t-value t_{95} is chosen instead of a z-value since n < 30 and the t-value equals $t_{95} = 2.445$.

The ratio between oven-dried and air-dried weight was assumed to be constant for the entire sample. For all samples, this ratio had a mean value of 0.917 with a standard deviation of 0.003. Hence the assumption that this ratio was constant for all samples was seen as valid, and its effect on the confidence interval of the biomass was therefore neglected.

Table 12. Raw data for biomass and vegetation height for each sampling point, as well as mean values, standard deviations and confidence interval for each vegetation type. The column called "95 % CI" denotes the second term in the equation for CI shown above, i.e. the deviation from the mean that makes up the 95 % CI.

Sample point	Height (cm)	Air-dry weight (g)	Oven-dry weight (g)	Oven-dry biomass (g/m^2)	Mean biomass (g/m^2)	St dev (g/m^2)	95 % CI	Mean height (cm)	St dev (cm)	95 % CI
RL19	150	226.8	208.1	832.5	1274.6	495.6	458.4	158.1	25.8	23.8
RL20	180	381.5	350.1	1400.3						
RL14	180	405.6	372.2	1488.7						
RL3	170	582.2	534.2	2136.9						
RL16	107	180.6	165.7	662.9						
RL35	150	270	247.8	991.0						
RL36	170	384.2	352.5	1410.2						
RH21	233	645.6	592.4	2369.6	1743.9	702.2	649.5	213.0	22.9	21.2
RH1	223	380.4	349.1	1396.2						
RH15	245	388.9	356.9	1427.4						
RH18	215	812.7	745.7	2983.0						
RH30	185	318.5	292.3	1169.0						
RH37	205	287.1	263.4	1053.8						
RH38	185	492.7	452.1	1808.4						
GH2	42	135	123.9	495.5	530.7	174.4	161.3	36.1	10.2	9.4
GH23	40	212	194.5	778.1						
GH17	43	156	143.1	572.6						
GH25	30	79	72.5	290.0						
GH24	50	133	122.0	488.2						
GH9	25	195	178.9	715.7						
GH8	23	102.1	93.7	374.8						
MH7	6	48.4	44.4	177.7	144.2	51.3	47.5	8.6	5.1	4.7
MH6	20	57.2	52.5	210.0						
MH5	6	38.5	35.3	141.3						
MH31	8	19.3	17.7	70.8						
MH32	6	38.4	35.2	140.9						
MH33	6	23.3	21.4	85.5						
MH34	8	49.9	45.8	183.2						

A4 Comparison with Other Studies

Table 13 below summarizes the biomass and vegetation height used to calculate wave damping according to the biomass method. Biomass for *Spartina anglica* and *Puccinellia maritima* were estimated from Bouma et al. (2010), vegetation heights for these species were taken from Rupprecht et al. (2015). Biomass for *Elymus athericus* is also taken from Rupprecht et al. (2015), vegetation height for this species is from Möller et al. (2014). Only mean values were used in the calculations. A MATLAB script was used to perform the calculations, see Appendix A5.2.

Table 13. Species characteristics.

Species	Biomass (g/m^2)	Vegetation height (cm)
Spartina anglica	360	27.9
Puccinellia maritima	330	23.3
Elymus athericus	600	70.0

A5 Code

A5.1 Python Script

Script used to calculate wave damping in the case study. Outputs are included to illustrate the results returned when running the script.

Wave Damping Script

Created for Master Thesis in Water Resources Engineering

By Timothy Ley (Spring 2021)

Program to calculate wave damping based on the biomass method by Maza et al. (2020). The program is run by importing CSV-files of SWL scenarios, wave scenarios and data generated in QGIS.

In [1]:
```
#To display multiple outputs:
from IPython.core.interactiveshell import InteractiveShell
InteractiveShell.ast_node_interactivity = 'all'
```

Import CSV-files

In [2]:
```
#Imort data analysis tool (Pandas)
import pandas as pd

#To determine if the script is to be run for case study (GIS data) or acedemic case (manually entered data):
while True:
    case=input('Select to run script for "Site" or "Hypothetical": ')

    if case=='Site':
        #Read data (OBS! Path is in local foder)
        data = pd.read_csv('Site_GIS_veg_1m.csv')               #Import QGIS data; segment length 1m
        scenario = pd.read_csv('Site_SWL_Scenario.csv')           #Import scenario definitions
        waves_in= pd.read_csv('Site_Incident_Waves_Examples.csv')  #Import wave inputs
        break

    elif case=='Hypothetical':
        data = pd.read_csv('Hypothetical_veg.csv')                    #Import data
        scenario = pd.read_csv('Hypothetical_SWL_Scenario.csv')           #Import scenario definitions
        waves_in= pd.read_csv('Hypothetical_Incident_Waves_Examples.csv')  #Import wave inputs
        break

    else:
        print('"Site" or "Hypothetical" was not enetered correctly, try again')

#Sort by selected columns
data=data.sort_values(by=['Transect_n','distance'])
data=data.reset_index(drop=True)   #Reset the indexing to match sorted indexing

#Preview the data
print(f'\033[1m GIS Data \033[0m')
data.head() #Show first five lines

print(f'\033[1m Scenario Data \033[0m')
scenario

print(f'\033[1m Wave Data \033[0m')
waves_in
```

```
Select to run script for "Site" or "Hypothetical": Site
 GIS Data
```

Out[2]:

	Transect_n	distance	Topografi	Vegetation_Type	Statistical Values_Biomass (g/m2)	Statistical Values_Height (m)
0	1	0	0.286488	NaN	NaN	NaN
1	1	1	0.281960	Reed_Low	1274.6	1.581
2	1	2	0.281960	Reed_Low	1274.6	1.581
3	1	3	0.297642	Reed_Low	1274.6	1.581
4	1	4	0.297642	Reed_Low	1274.6	1.581

```
 Scenario Data
```

Out[2]:

	Scenario	RH2000 (m)
0	Today, 100	1.53
1	2050, 100	1.63
2	2100, 100	2.17

```
 Wave Data
```

Out[2]:

	Wave/Scenario	H1	L1	H2	L2	H3	L3
0	Maximum H and L	1.0998	24.938	1.2714	26.7266	1.599	29.7877

Calculations

In [3]:

```
##TIME
import time
start = time.time()

                        ###################### DESCRIPTION ######################
# The script iterates in the following order: Wave Scenario -> Sea Level Scenario -> Transect number -> Segment.
# When the last step is completed looping, the previous step is looped and so on till all scenarios have been looped.

# Please note: Water level scenarios should be given in RH2000 (topography in RH2000).

#Select iteration method
method=input('Select method (h0, m, x=0 or original): ')

######List creation#######
#All indicating "All" scenarios
#Transect=Final H-value of transect; Segment=Each H-value along transect
H_All_Transect = []      #All final transect wave heights
H_All_Segment = []       #All segment wave heights
H_Segment = []           #Segment wave heights
Beta_All_Segment = []    #All segment damping coefficents
Beta_Segment = []        #Segment damping coefficents

for row in range(0,len(waves_in)):           #Goes trough rows in waves_in for each scenario
    for scenario_nr in range(1,len(scenario)+1): #Each scenario (changes input for: water depth(RH2000) and incomming wave
                                                 #(H and L))
        #List for each scenario
        H_Transect = []         #Creates and empties list for each new scenario

        for k in range(0,len(data)):     #Goes through every row/segment in GIS data

            #If start of a new transect
            if data['distance'][k]==0.0:

                #Boundry conditions for each transect
                H_0= waves_in[f'H{str(scenario_nr)}'][row]  #H_0 is incomming wave
                L= waves_in[f'L{str(scenario_nr)}'][row]    #L is incomming wave and assumed constant along transect
                x= data['distance'][k]                      #Sets the first distance to 0
                m=0                                         #In case m-method is used
                H= H_0
                beta= 0
                if case=='Site':
                    topo=0.12               #Sets the topography of each start of transect too 0.12 (due too RH2000).
                                            #Thereby topography info in GIS for first point is overridden/not included
                elif case=='Hypothetical':      # In the hypothetical case topo=0 and is constant since sea level/flume level
                    topo=0                  #is given relative to the surface,and not as RH2000

            #If next point along the transect
            else:

                #If previous segment was: Topography > sea level --> the following loop is not performed.
                # Will not be true until new transect
                if H!=0:
                    #No wavedamping calculation if biomass=0
                    if data['Statistical Values_Biomass (g/m2)'][k]==0:
                        topo = data['Topografi'][k]  #So that the next transect obtaines the correct avarage topography
                        H_Segment.append(round(H,4))  #H remains the same as previous segment
                        beta=0                        #Wave damping coefficent=0
                        Beta_Segment.append(round(beta,4))

                    #If all OK
                    else:
                        h_veg = data['Statistical Values_Height (m)'][k] #Height vegetation (m)
                        topo_prev = topo    #Topography of previous segment end-point
                        topo = data['Topografi'][k]  #Topography of current segment end-point
                        topo_avrg = (topo_prev+topo)/2  #Topography avarage between segment endpoints
                        sea_lev = scenario['RH2000 (m)'][scenario_nr-1] #Seawater level in RH2000 for scenario
                        h_water = sea_lev-topo_avrg        #Water depth

                        #If h_water<0 (no water) or H<=0 no wave, H=0 is saved to results:
                        if topo_avrg>=sea_lev or topo>=sea_lev or H=='N/A' or H<=0:
                            H=0
                            beta=0
                            H_Segment.append(H)
                            Beta_Segment.append(beta)
                            continue                    #End loop

        #If all criteria are ok -->
                        else:
                            if h_veg>h_water:
                                SR=1          #If the plant is submerged the submergance ratio is 1
                            else:
                                SR=h_veg/h_water
                            SB = (data['Statistical Values_Biomass (g/m2)'][k]/h_veg)*min(h_veg,h_water)*SR #Standing biomass
                            VSB = SB/h_water                #Volumetric standing biomass
                            L_v = 1                        #Vegetation lenght unit
                            LR = L_v/L                      #Vegetation unit/wave length
                            if data['distance'][k]%10==0 or H==H_0:    #H_i is updated every 10m
                                H_i=H
                            HB = VSB * LR * H_i/h_water      #Hydraulic biomass

                #Select Eq. for damping coefficent beta (Maza or the fit in this thesis)
                            beta=0.0122*(HB**0.6858)         #New fit - Damping coefficient
                            #beta = 9.2*10**(-4)*HB+0.10     #Maza fit - Damping coefficient

                #Iteration method
```

```
                            #H0 method:
                            if method=='h0':
                                H_0 = H*(1+beta*x)              #New H_0 based on pervious x and H
                                x = data['distance'][k]         #Distance = cross shore distance
                                H = H_0/(1+beta*x)              #Final result for each segment along transect

                            #m-method
                            elif method=='m':
                                m = H-(H_0/(1+beta*x))        #m-value
                                x = data['distance'][k]       #Distance = cross shore distance
                                H = H_0/(1+beta*x) + m        #Final result for each segment along transect

                            #x=0 at start of each segment --> x=1 at end of segment (Like Foster-Martinez et al. (2020))
                            elif method=='x=0':
                                H_0 =H
                                x = 1                           #Distance 1m
                                H = H_0/(1+beta*x)              #Final result for each segment along transect

                            #Like original Eq. by Dalrymple (1984), but beta update (causes discontinuities)
                            elif method=='original':
                                x = data['distance'][k]          #Distance = cross shore distance
                                H = H_0/(1+beta*x)              #Final result for each segment along transect

        #Saving segment results
            if type(H)==str or H<=0:
                H_Segment.append(0)        #Appends the wave height
                Beta_Segment.append(0)     #Appends damping coefficent
            else:
                H_Segment.append(round(H,4))        #Appends the wave height, 4 digits
                Beta_Segment.append(round(beta,4))   #Appends damping coefficent, 4 digits

        #When the entire transect has been completed results are saved to lists
            if k==len(data)-1 or data['Transect_n'][k] != data['Transect_n'][k+1]:
                    H_Transect.append(round(H,4))         #Final value of H for each transect
                    H_All_Segment.append(H_Segment)
                    H_Segment=[]                          #Empties list for each new scenario

                    Beta_All_Segment.append(Beta_Segment)
                    Beta_Segment=[]

    #Final transect results
        H_All_Transect.append(H_Transect)    #Gathers all transects, waves and scenarios

##TIME
end = time.time()
print(f'\n Time: {end - start} s')
```

```
Select method (h0, m, x=0 or original): h0

 Time: 3.442887306213379 s
```

Show and save results

In [4]:
```
#Wave height and damping coefficent per meter along each transect

#Set up multiple index for dataframe
iterables = [waves_in['Wave/Scenario'], scenario['Scenario'], data['Transect_n'].unique()]
multi = pd.MultiIndex.from_product(iterables, names=['Wave', 'Scenario', 'Transect'])

#Create dataframe
df_Beta_All=pd.DataFrame(Beta_All_Segment, index =multi)
df_H_All=pd.DataFrame(H_All_Segment, index =multi)

#Save dataframe to CSV-file
df_Beta_All.to_csv('Beta_All.csv')
df_H_All.to_csv('H_All.csv')

#Show dataframe with wave heights
print('H')
df_H_All
```

H

Out[4]:

Wave	Scenario	Transect	0	1	2	3	4	5	6	7	8	9	...	232	233	234	235	236	237
Maximum H and L	Today, 100	1	1.0998	0.9853	0.8891	0.8098	0.7432	0.6862	0.6368	0.5935	0.5555	0.5220	...	NaN	NaN	NaN	NaN	NaN	NaN
		2	1.0998	0.9802	0.8767	0.7935	0.7249	0.6674	0.6182	0.5755	0.5384	0.5057	...	0.0610	0.0608	0.0605	0.0603	0.0601	0.0599
		3	1.0998	0.9898	0.9008	0.8247	0.7589	0.7011	0.6499	0.6046	0.5642	0.5290	...	NaN	NaN	NaN	NaN	NaN	NaN
		4	1.0998	0.9863	0.8900	0.8096	0.7415	0.6832	0.6332	0.5898	0.5518	0.5184	...	NaN	NaN	NaN	NaN	NaN	NaN
	2050, 100	1	1.2714	1.1388	1.0277	0.9361	0.8592	0.7934	0.7364	0.6866	0.6427	0.6041	...	NaN	NaN	NaN	NaN	NaN	NaN
		2	1.2714	1.1333	1.0144	0.9187	0.8397	0.7734	0.7166	0.6674	0.6245	0.5867	...	0.0802	0.0799	0.0796	0.0793	0.0790	0.0787
		3	1.2714	1.1435	1.0402	0.9519	0.8759	0.8092	0.7503	0.6982	0.6519	0.6115	...	NaN	NaN	NaN	NaN	NaN	NaN
		4	1.2714	1.1399	1.0287	0.9359	0.8574	0.7902	0.7326	0.6826	0.6388	0.6002	...	NaN	NaN	NaN	NaN	NaN	NaN
	2100, 100	1	1.5990	1.4872	1.3825	1.2910	1.2103	1.1373	1.0711	1.0109	0.9559	0.9066	...	NaN	NaN	NaN	NaN	NaN	NaN
		2	1.5990	1.4767	1.3545	1.2524	1.1651	1.0896	1.0228	0.9633	0.9101	0.8624	...	0.1971	0.1965	0.1959	0.1953	0.1947	0.1941
		3	1.5990	1.4552	1.3360	1.2332	1.1436	1.0644	0.9940	0.9313	0.8750	0.8254	...	NaN	NaN	NaN	NaN	NaN	NaN
		4	1.5990	1.4893	1.3845	1.2902	1.2054	1.1288	1.0607	0.9998	0.9451	0.8957	...	NaN	NaN	NaN	NaN	NaN	NaN

12 rows × 242 columns

In [5]:
```
#Wave height at the end of each transect

#Set up multiple index for dataframe
iterables = [waves_in['Wave/Scenario'], scenario['Scenario']]
multi = pd.MultiIndex.from_product(iterables, names=['Wave', 'Scenario'])

#Create dataframe
df_H_FINAL=pd.DataFrame(H_All_Transect, index =multi, columns =data['Transect_n'].unique())

#Save dataframe to CSV-file
df_H_FINAL.to_csv('H_Transect_End_Point.csv')

#Shows the dataframe for end of transect
df_H_FINAL

                                    ###############Script end########################
```

Out[5]:

Wave	Scenario	1	2	3	4
Maximum H and L	Today, 100	0.2789	0.0590	0.1579	0.1359
	2050, 100	0.3298	0.0776	0.1866	0.1582
	2100, 100	0.5494	0.1917	0.2856	0.2498

A5.2 MATLAB Scripts

The following script defines a function that was used to calculate the wavelengths at two known depths of a wave with known period. It is based on approximations provided by (Nielsen, 2009) and is used in several other scripts.

```
function L = WaveL(T,h)
%This function returns the wavelengths of a wave with a known period at two
%known depths h =[h1 h2].

Lo = (9.81/(2*pi)).*T.^2;
koh = (2*pi./Lo).*h;
kh = zeros(size(koh));

%Approximating kh. The approximations are from Nielsen (2009).
for i = 1:length(koh)
    if koh(i) > 2
        kh(i) = koh(i)*(1+2*exp(-2.*koh(i)));
    else
        kh(i) = (koh(i).^0.5).*(1+(1/6).*koh(i)+(11/360).*koh(i).^2);
    end
end

L = 2*pi*h./kh;
```

The following script was used for calculating wave damping from the different vegetation types in the hypothetical cases.

```
%% Vegetation types
%This function returns the wave damping of high reed, low reed, high grass,
%and high meadow in percent for the specified depth h. The wave height and
%wavelength are the same as the base line scenario and are kept constant.
%In the script, the relationship between beta and HB is the new fit used in
%this thesis, not the original fit by Maza et al. (2020).

function y = Vegetation(h)
%% Hydrodynamic conditions
Ho = 0.18;
T = 4;
L = WaveL(T,0.5); %See previous script
Lv = 1;

%% Results from vegetation sampling
h_veg = [2.13 1.58 0.361 0.081];
mass = [1736.3 1274.4 530.5 145.0];

%% Beta parameters
SR = zeros(1,length(h_veg));
for i = 1:length(h_veg) %SR criteria
    if h_veg(i) > h
        SR(i) = 1;
    else
        SR(i) = h_veg(i)/h;
    end
end

SB = (mass./h_veg).*min(h_veg,h).*SR;
LR = Lv./L;
HB = (SB/h).*LR.*Ho./h;
beta = 0.0122*HB.^(0.6058);

%% Plot
x = 0:0.1:10;
y = zeros(length(x),length(beta));

for i = 1:length(x)
    for j = 1:length(beta)
        y(i,j) = 1/(1+beta(j)*x(i));
    end
end
end
```

The following scripts are functions that were used to calculate the influence on wave damping of the different β-parameters.

```
function y = Damping_m(mass)
%Returns wave damping in percent as a function of biomass.
hv = 1.58;
h = 0.5;
L = 8.6729;
Lv = 1;
Ho = 0.18;
x = 10;

SR = zeros(1,length(h));
for i = 1:length(h)
    if hv > h(i)
        SR(i) = 1;
    else
        SR(i) = hv/h(i);
    end
end

b_m = 0.0122.*((mass./hv).*min(hv,h).*SR.*(1./h).*(Lv./L).*(Ho./h)).^0.6058;
y = 100*(1-1./(1 + x.*b_m));


function y = Damping_H(Ho)
%Returns wave damping in percent as a function of incident wave height Ho.
mass = 1274.6;
hv = 1.58;
h = 0.5;
L = 8.6729;
Lv = 1;
x = 10;

SR = zeros(length(h),1);
for i = 1:length(h)
    if hv > h(i)
        SR(i) = 1;
    else
        SR(i) = hv/h(i);
    end
end

b = 0.0122.*((mass./hv).*min(hv,h).*SR.*(1./h).*(Lv./L).*(Ho./h)).^0.6058;
y = (1-1./(1 + x.*b))*100;
```

```
function y = Damping_d(h)
%Returns wave damping in percent as a function of water depth.
mass = 1274.6;
hv = 1.58;
Ho = 0.18;
L = 8.6729;
Lv = 1;
x = 10;

d = length(h); %Returns the number of different h values
SR = zeros(1,d);
for i = 1:d
    if hv > h(i)
        SR(i) = 1;
    else
        SR(i) = hv/h(i);
    end
end

b = 0.0122.*((mass./hv).*min(hv,h).*SR.*(1./h).*(Lv./L).*(Ho./h)).^0.6058;
y = (1-1./(1 + x.*b))*100;


function y = Damping_hv(hv)
%Returns wave damping in percent as a function of water depth.
mass = hv.*(1274.6/1.58); %Constant density
h = 0.5;
Ho = 0.18;
L = 8.6729;
Lv = 1;
x = 10;

d = length(hv); %Returns the number of different hv values
SR = zeros(1,d);
for i = 1:d
    if hv(i) > h
        SR(i) = 1;
    else
        SR(i) = hv(i)/h;
    end
end

b = 0.0122.*((mass./hv).*min(hv,h).*SR.*(1./h).*(Lv./L).*(Ho./h)).^0.6058;
y = (1-1./(1 + x.*b))*100;
```

```
function y = Damping_L(L)
%Returns wave damping in percent as a function of wavelength.
mass = 1274.6;
hv = 1.58;
h = 0.5;
Lv = 1;
Ho = 0.18;
x = 10;

SR = zeros(1,length(h));
for i = 1:length(h)
    if hv > h(i)
        SR(i) = 1;
    else
        SR(i) = hv/h(i);
    end
end

b_m = 0.0122.*((mass./hv).*min(hv,h).*SR.*(1./h).*(Lv./L).*(Ho./h)).^0.6058;
y = 100*(1-1./(1 + x.*b_m));
```

The functions above were plotted in a separate script where the parameters were plotted in the following intervals:

Biomass: 0 – 2000 g/m^2

H_o: 0 – 1.5 m

h: 0 – 3 m

h_{veg}: 0 – 2 m

L: 0 – 50 m

Note that in the scripts, H_o signifies the wave height at x = 0 m. In other words, it is the incident wave height and not the deep-water wave height.

The following script was used in the sensitivity analysis, in the SR bar chart and to compare the biomass method with damping observed by Möller et al. (2014) and Bouma et al. (2010).

```
%% Wave damping
%This script allows the user to enter wave conditions and vegetation
%characteristics to calculate the wave height reduction in percent. This
%script was used to calculate wave damping in the sensitivity analysis as
%well as to compare the biomass method with observed wave damping from
%Bouma et al. (2010) and Möller et al. (2014).
%The script uses the exponential relation between beta and HB as defined in
%the thesis, not the linear relation as defined by Maza et al. (2020).

%% Wave conditions
Ho = 0.18;
T = 4;
h = 0.5;
L = WaveL(T,0.5);
Lv = 1;

%% Vegetation characteristics
hv = 0.25;
m = (144.2/0.086).*hv; %Ensures constant biomass density

%% Beta parameters
LR = Lv./L;
SR = hv./h;
if hv > h
    SR = 1;
end

HB =(((m./hv)*min(hv,h)*SR./h)*LR*Ho./h);
x = 10;
beta = 0.0122*HB^0.6058;
H2=Ho./(1+x*beta);

%% Wave height reduction in percent
Reduction = 100*(Ho-H2)/Ho;
```

The following script was used to calculate incident wave heights at the shoreline from the wave time series referred to in section 4.4.2.

```
function Waves = Transform(Data,Scenario)
%This function transforms deep water waves to waves at the edge of the
%coastal meadows. Inputs are the wave time series, called Data, and the
%water depth at the edge of the salt meadows in the different scenarios,
%called Scenario. Output is a 4 column time series of wave height H,
%wavelength at shoreline L2, deep water wavelength Lo and the significant
%period Ts. Scenario depths should be given relative to mean sea
%water level, not in RH2000.
%Approximations of L from koh are based on Nielsen (2009).

%% Extracting data from time series
Hs = Data(:,2); % Hmo = Hs
Ts = 0.95*Data(:,3); % Ts = 0.95*Tp
do = Data(:,5)-0.12; % Subtract 12 cm to convert depth in RH2000 to depth
%relative to current (2021) mean sea water level.
theta = Data(:,4);
d2 = Scenario;

%% Wavelengths
Lo = (9.81/(2*pi)).*Ts.^2;
d1 = do + d2;

koh1 = 2*pi.*d1./Lo;
koh2 = 2*pi.*d2./Lo;
kh1 = zeros(size(koh1));
kh2 = zeros(size(koh2));

%Observe that the author defines upper statement for koh>1.75 and lower for
%koh<2.72, so the two overlap in the range 1.75<koh<2.72. Here koh>2 is
%chosen as a separation of the two methods.
for i = 1:length(koh1)
    if koh1(i,1) > 2
        kh1(i,1) = koh1(i,1).*(1+2*exp(-2.*koh1(i,1)));
    else
        kh1(i,1) = (koh1(i,1).^0.5).*(1+(1/6).*koh1(i,1)+(11/360).*koh1(i,1).^2);
    end
end

for i = 1:length(koh2)
    if koh2(i,1) > 2
        kh2(i,1) = koh2(i,1).*(1+2*exp(-2.*koh2(i,1)));
    else
        kh2(i,1) = (koh2(i,1).^0.5).*(1+(1/6).*koh2(i,1)+(11/360).*koh2(i,1).^2);
    end
end

L1 = 2*pi.*d1./kh1;
L2 = 2*pi.*d2./kh2;
```

```
%% Shoaling
C1 = L1./Ts;
C2 = L2./Ts;
n1 = 0.5*(1 + (4*pi.*(d1./L1))./(sinh(4*pi.*(d1./L1)))); %Airy theory
n2 = 0.5*(1 + (4*pi.*(d2./L2))./(sinh(4*pi.*(d2./L2))));

%Shoaling coefficient
KS = sqrt((n1./n2).*(C1./C2));

%% Refraction
%Preallocate vector size for alpha0
alpha0 = zeros(length(Data),1);

% This loop transforms wave direction theta into an incident angle
% which can be used in Snell's law.
for i=1:length(theta)
    theta = Data(i,4); % Wave direction as defined by compass degrees
    if(270 < theta(i) && theta(i) <= 360)
        alpha0(i,1) = theta(i) - 270;
    elseif(180 < theta(i) && theta(i) <= 270)
        alpha0(i,1) = 270 - theta(i);
    else
        alpha0(i,1) = 90;
        %this means cos(alpha0) = 0, so that KR = 0. We want
        %this because theta in this range means the waves come from the
        %east, in other words the waves travel away from the shore, so Hi
        %should be zero.
    end
end

alpha2 = (180/pi)*asin((C2./C1).*sin(alpha0.*pi./180));
%Observe the transformation into rad and then back to degrees

%Refraction coefficient
KR = sqrt(cos(alpha0.*pi./180)./cos(alpha2.*pi/180));

%% Incident wave height
Hi = Hs.*KS.*KR;

%Breaking wave condition
for i = 1:length(Hi)
    if Hi(i) > 0.78*d2
        Hi(i) = 0.78*d2;
    end
end

Waves = [Hi,L2,Lo,Ts];
end
```